

Non-equilibrium dynamics in warm dense matter by Free Electron Laser radiation



Keisuke Hatada

Univ. Toyama

*TIMEX collaboration 2007-2013 - (ELETTRA resp.: C. Masciovecchio):
A. Di Cicco, F. Bencivenga, R. Cucini, F. D'Amico, S. Di Fonzo, A.
Filipponi,
E. Giangrisostomi, R. Gunnella, E. Principi, L. Properzi, A. Trapananti*



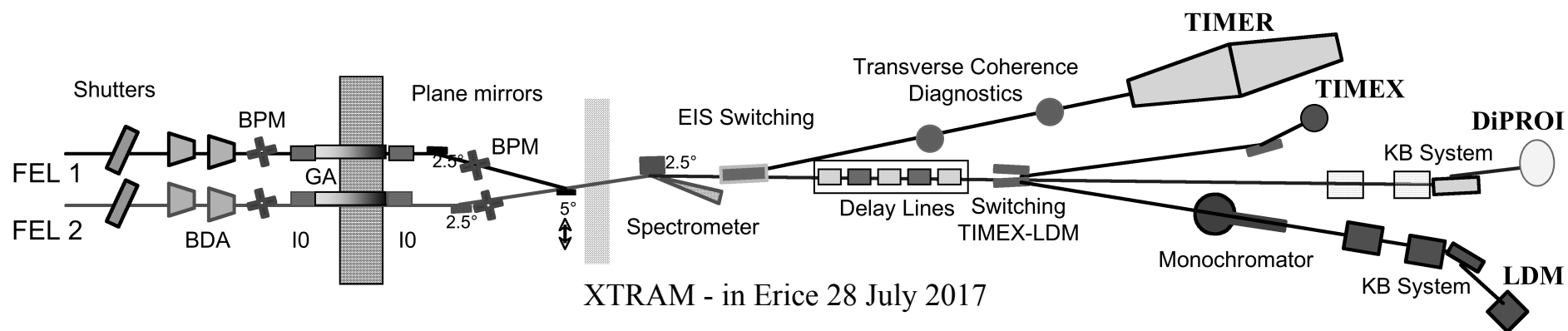
Fermi@Elettra FEL in Trieste

The FEL1 source is presently operating (~routine operation started in Dec 2012, FEL2 in 2014).

- [E. Allaria et al., New Journal of Physics 14 \(2012\) 113009](#)

The FEL1/FEL2 photon beams are delivered to the beamlines through the PADReS (Photon Analysis Delivery and Reduction System). This includes gas monitor detectors and attenuators, mirror switching, x-ray spectrometers. TIMEX is an end-station developed through a collaboration between the Univ. of Camerino and ELETTRA (EIS).

Parameter	FEL - 1	FEL - 2	Units
Wavelength	100 - 20	20 - 3	nm
Photon Energy	12 - 62	62 - 413	eV
Pulse Length	30 - 100	< 100	fs
Bandwidth	~ 20 - 40	~ 20 - 40	meV
Polarization	variable	variable	-
Repetition Rate	10 - 50	10 - 50	Hz
Peak Power	1 ÷ 5	~ 1	GW
Photons per Pulse	$2 \cdot 10^{14}$ @ 100 nm	$1 \cdot 10^{13}$ @ 10 nm	-
Power Fluctuation	~ 25%	> 50%	-
Central Wavelength Fluctuation	within bandwidth	within bandwidth	-
Output Transverse Position Fluctuation	50	50	µm
Pointing Fluctuation	< 5	< 5	µrad
Output Spot Size (intensity, FWHM@waist)	290	140	µm
Divergence (intensity, RMS)	50 @ 40 nm	15 @ 10 nm	µrad





TIMEX

project (<http://gnxas.unicam.it/TIMEX>)

- **TIMEX** end-station proposal (2006): **T**ime-resolved studies of **M**atter under **E**Xtreme and metastable conditions
See report on Notiziario Neutroni e Luce di Sincrotrone 26 Volume 18 n. 2 (July 2013)
- EIS beamline including TIMEX approved (UniCam-ELETTRA agreement 2007-2013)

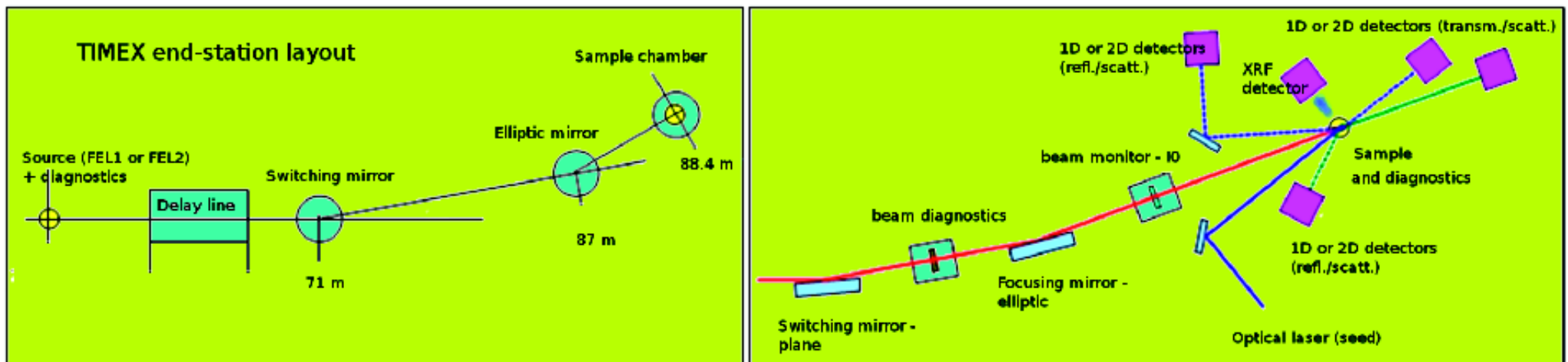


Figure 1

Sketch of the TIMEX end-station under commissioning at the FERMI@Elettra FEL facility. The left side shows the main components of the beamline, including the delay line and the elliptic mirror that should be installed after a performance test, within a few months. In the right side, we show some details of the focusing and aligning devices and the detectors used for reflection, transmission, scattering and x-ray emission (XRF) measurements using both FEL and optical laser pulses. The pump-probe scheme should be tested within a few months.

XTRAM - in Erice 28 July 2017

TIMEX end-station: timeline and status

- Design of the end-station and place of orders completed in June 2010. Vacuum chambers delivered in late October 2010. Pilot experiments (2007-2010) completed. Assembling and test of the main components of the TIMEX end-station in the main Fermi hall started in December 2010.
- Problems: the TIMEX optics (C. Svetina, D. Cocco) did not match specifications (SESO manufacturing) and are still under construction. All tests and first runs (for a total of ~3 weeks of beamtime) since March 2011 using a simplified optics.
- Beamline open to users since the first call for proposals. Optics delivered and installed in late 2013, pump-probe (laser-seed + FEL) installed and tested (late 2013).
- Personnel/contacts: C. Masciovecchio group (main responsible E. Principi)

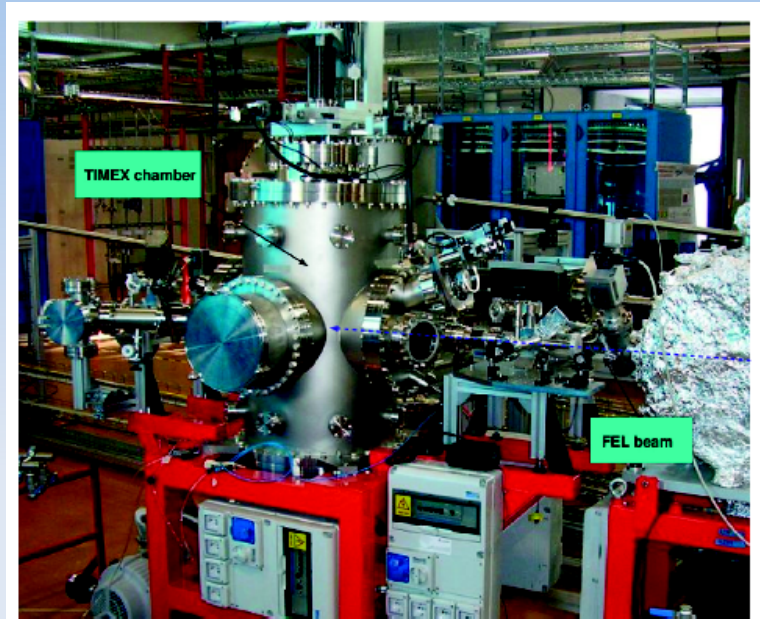
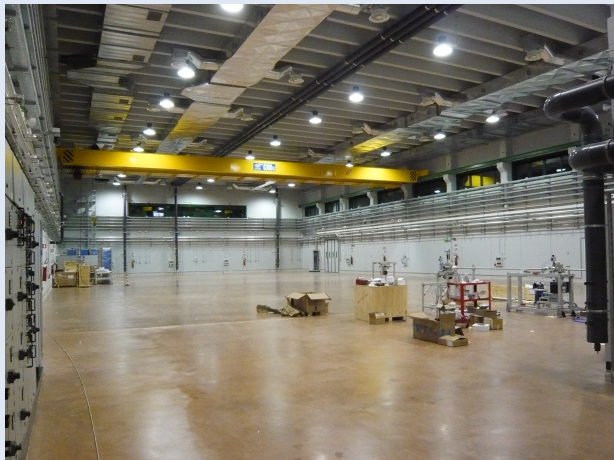


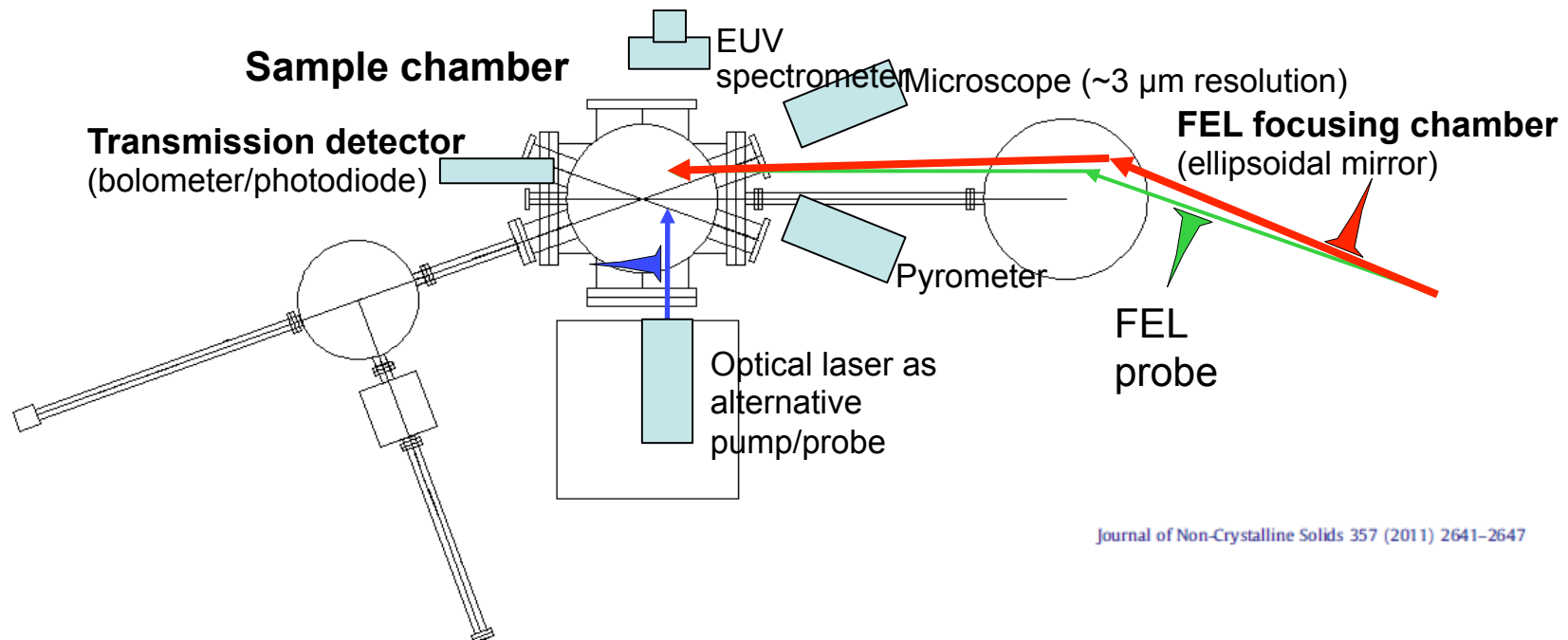
Figure 2

Picture of the TIMEX chamber installed and aligned at the exit of the FEL1 source in 2012. The FEL beam (blue dashed line, guide for the eye) has been aligned up to the main TIMEX chamber, where the sample position can be controlled with a 5-axis motorized manipulator while the transmitted and reflected pulses were measured by the photodiodes and thermopiles.



Assembling the TIMEX UHV chamber in the main -empty- Fermi hall (17 nov 2010)

TIMEX layout details



Journal of Non-Crystalline Solids 357 (2011) 2641–2647

Probing phase transitions under extreme conditions by ultrafast techniques:
Advances at the Fermi@Elettra free-electron-laser facility

Invited Paper

Andrea Di Cicco^{a,b,c,*}, Francesco D'Amico^b, Goran Zgrablic^b, Emiliano Principi^a, Roberto Gunnella^a,

Damage to VUV, EUV, and X-ray Optics III, edited by Libor Juha, Saša Bajt, Richard A. London,
Proc. of SPIE Vol. 8077, 807704 · © 2011 SPIE · CCC code: 0277-786X/11/\$18 · doi: 10.1117/12.887833

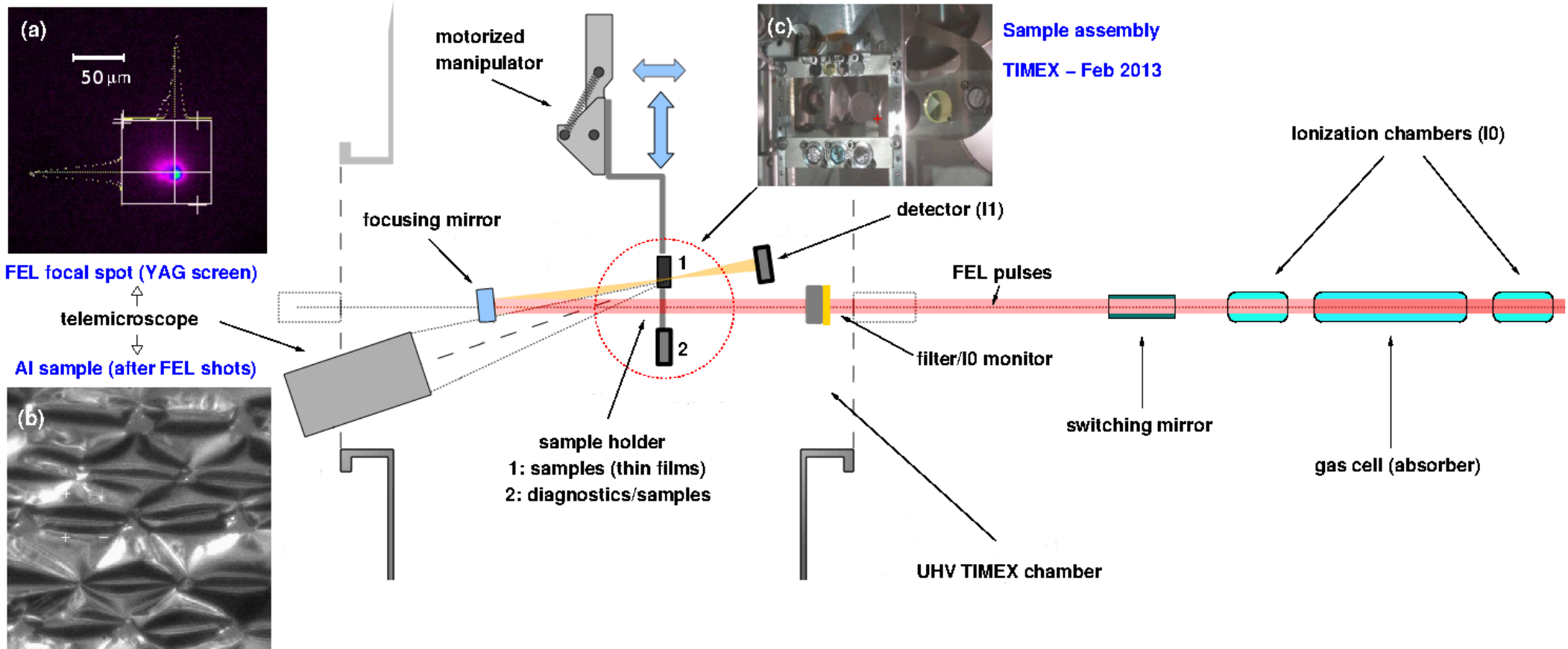
Probing matter under extreme conditions at FERMI@Elettra: the TIMEX beamline

Andrea Di Cicco^a, Filippo Bencivenga^b, Andrea Battistoni^b, Daniele Cocco^b,
Riccardo Cucini^b, Francesco D'Amico^b, Silvia Di Fonzo^b, Adriano Filipponi^c,
Alessandro Gessini^b, Erika Giangrisostomi^b, Roberto Gunnella^a,
Claudio Masciovecchio^b, Emiliano Principi^b, and Cristian Svetina^b

XTRAM in Erice 28 July 2017

- *The flexible set-up of the Timex end-station can host different experimental configurations.*
- *Details on the experimental layout and pilot pump and probe experiments are reported in the papers of the Timex collaboration*

Set-up for first experiments



Fluence and focusing

- Focusing provided by a spherical focusing mirror (metal or multilayer coating) with $\sim 10 \times 10$ mm best focus size, (normal reflection: loss of about 90% of fluence for soft x-ray photons). The mirror was a platinum-coated silicon mirror (400 mm radius of curvature, 0.2 nm roughness RMS) placed close to normal incidence (angle of incidence 3 degs). Maximum fluence in these conditions was about 20 J/cm^2 .

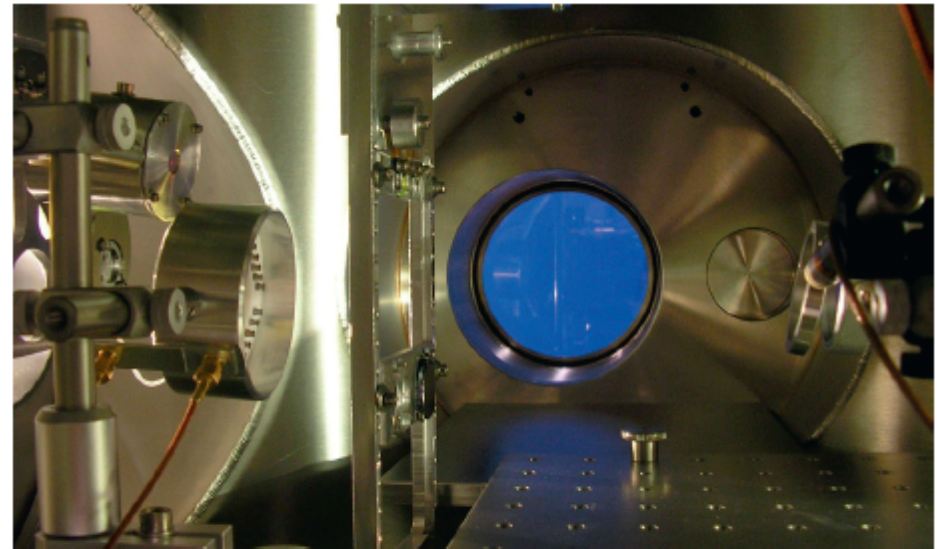
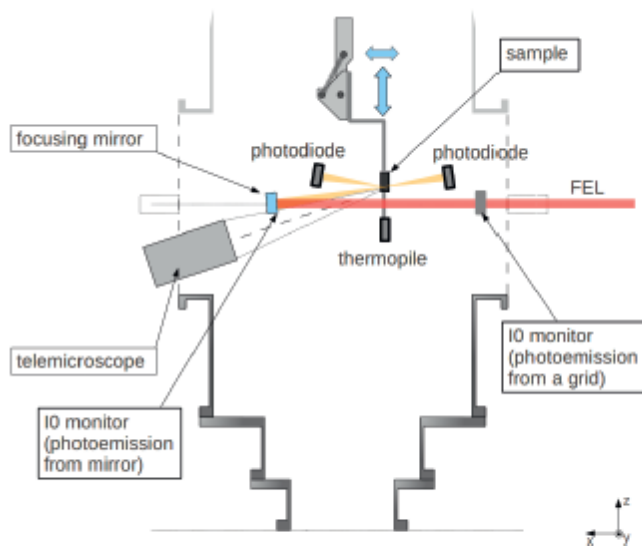


Figure 3

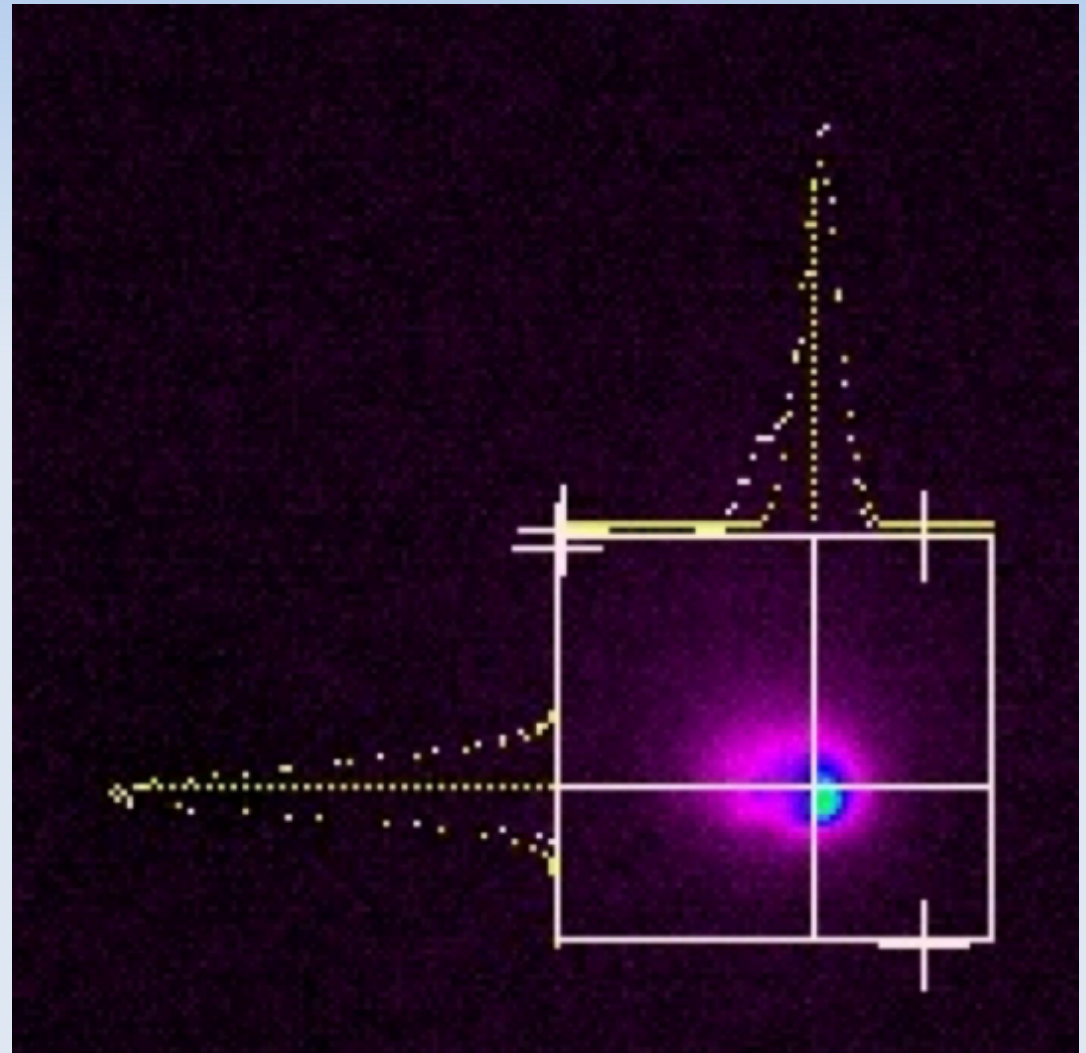
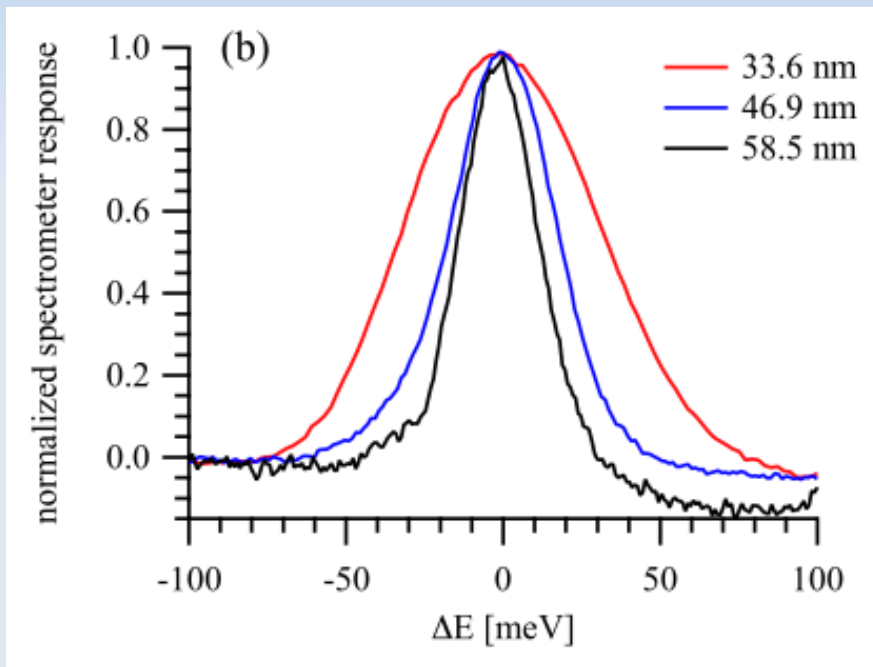
Left side: sketch of the current (March 2013) experimental set-up of the TIMEX chamber, including optics, detectors and diagnostics. Right side: picture of the setup including the sample holder (center), the Au grid (I₀ monitor) and a photodiode (left), and the focusing mirror (right).

Shape of the pulse

Seeded laser

Real space

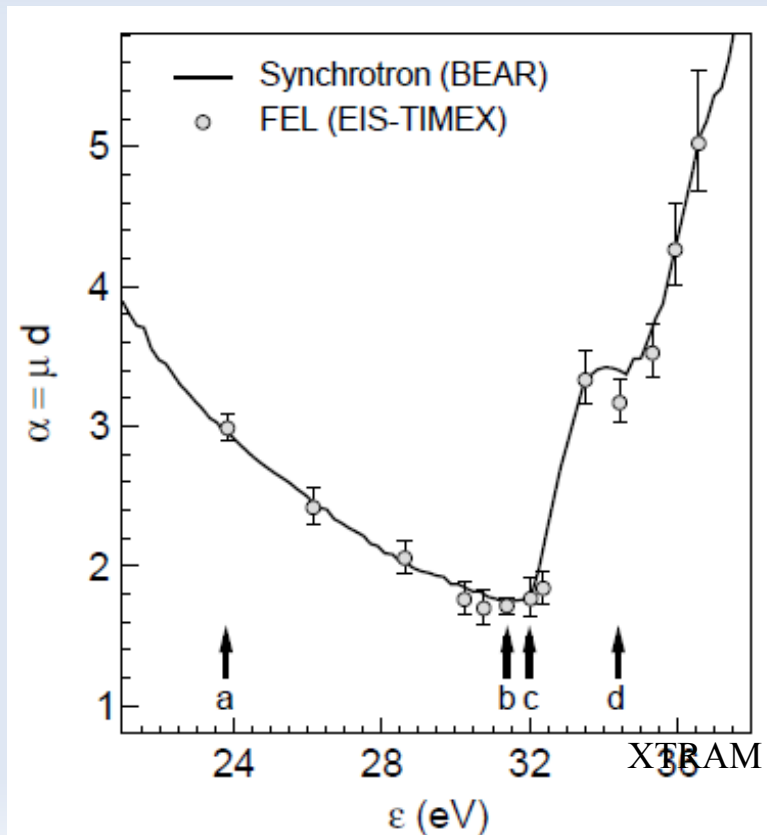
Energy space



Tunability across the edges

Tunability experiments at the FERMI@Elettra free-electron laser

- High-quality Ti $M_{2,3}$ -edge (3p) absorption spectra with FEL1 ultrashort pulses: near-edge changes at high fluence (high-energy density). E. Principi et al. (2013).



New Journal of Physics **14** (2012) 113009 (19pp)
Received 20 September 2012
Published 7 November 2012
Online at <http://www.njp.org/>
doi:10.1088/1367-2630/14/11/113009

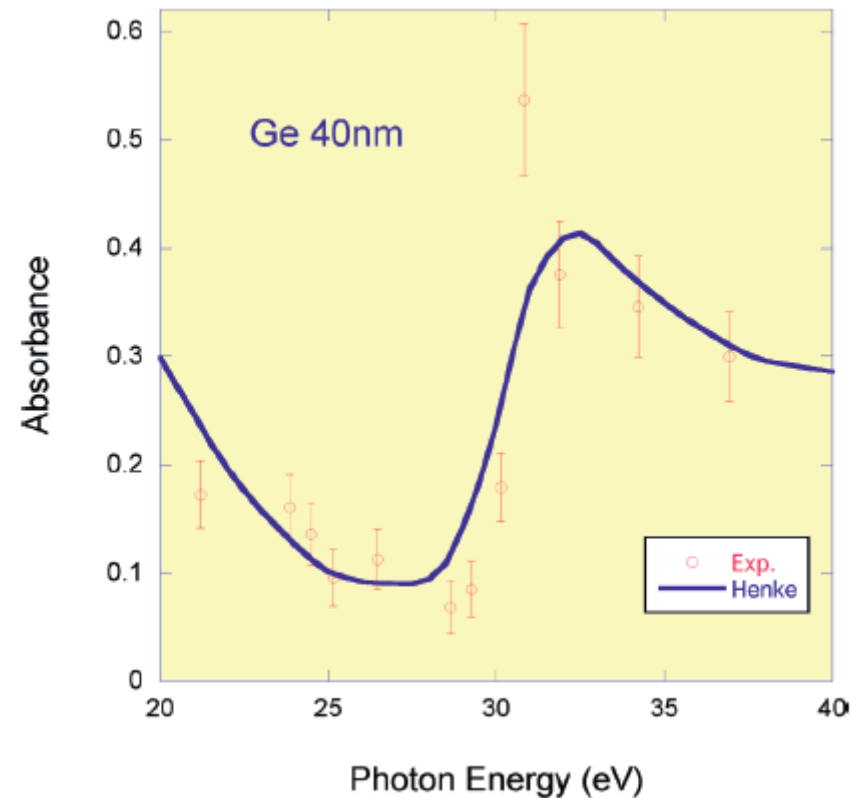


Figure 6

First near-edge $M_{4,5}$ x-ray absorption spectrum (dots with error bars) of Ge ultrathin foil collected at FERMI@Elettra,² compared with the calculated absorbance (blue line¹⁷).

Ultrafast excitation of the Si(100) surface: pictorial view

PHYSICAL REVIEW B 73, 134108 (2006)

Thermodynamic pathways to melting, ablation, and solidification in absorbing solids under pulsed laser irradiation

Patrick Lorazo,^{1,2} Laurent J. Lewis,^{2,*} and Michel Meunier^{1,7}

A combined MC and MD calculation on a (100) slab of 142560 atoms was used to calculate the thermodynamic pathway after excitation (500 fs pulse). Rapid non-thermal disordering and nearly isochoric heating (B) of the metallic liquid is followed by cooling in the liquid-vapor regime.

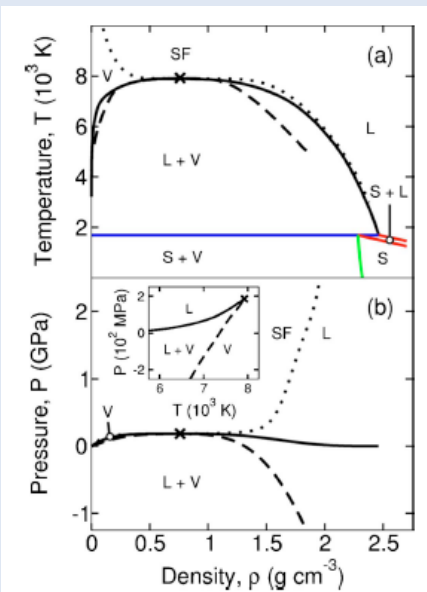


FIG. 3. (Color online) Phase diagram of silicon: (a) ρ - T plane; (b) ρ - P plane; inset: T - P plane. Black solid line: binodal (liquid-vapor coexistence); blue: triple line (solid-liquid-vapor coexistence); green: solid-vapor coexistence line; red: solid-liquid coexistence lines; dotted line: critical isobar and isotherm; dashed line: spinodal; cross: critical point. S: solid; L: liquid; V: vapor; SF: supercritical fluid (for $T > T_c$ and $P > P_c$). See text for details.

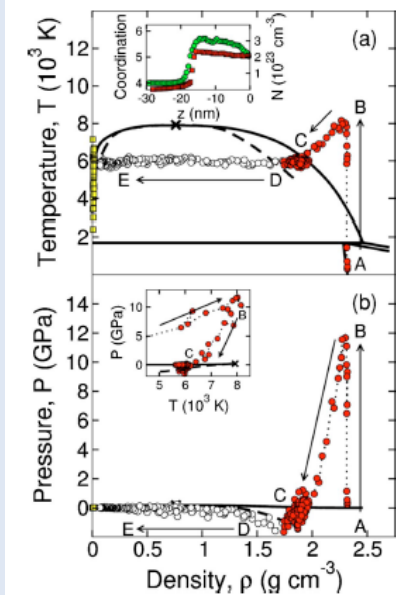


FIG. 5. (Color online) Time evolution of the system in the (a) ρ - T and (b) ρ - P planes for a 500 fs pulse at a fluence $F = F_{in}^{fs} = 0.225\ J\ cm^{-2}$; the trajectory is for a region of the target initially at a depth of 4 nm below the surface. White circles and dotted line: macroscopic branch; red circles: dense branch; yellow squares: gas branch. Arrows indicate the flow of time. Capital letters refer to locations in the phase diagram (see text). Insets: (a) coordination (green circles) and electron density N (red squares) as a function of distance from the surface z at $t = 1\ ps$ (note the change in properties across the solid-liquid interface at $z \approx -18\ nm$); (b) view of the trajectory in the T - P plane.

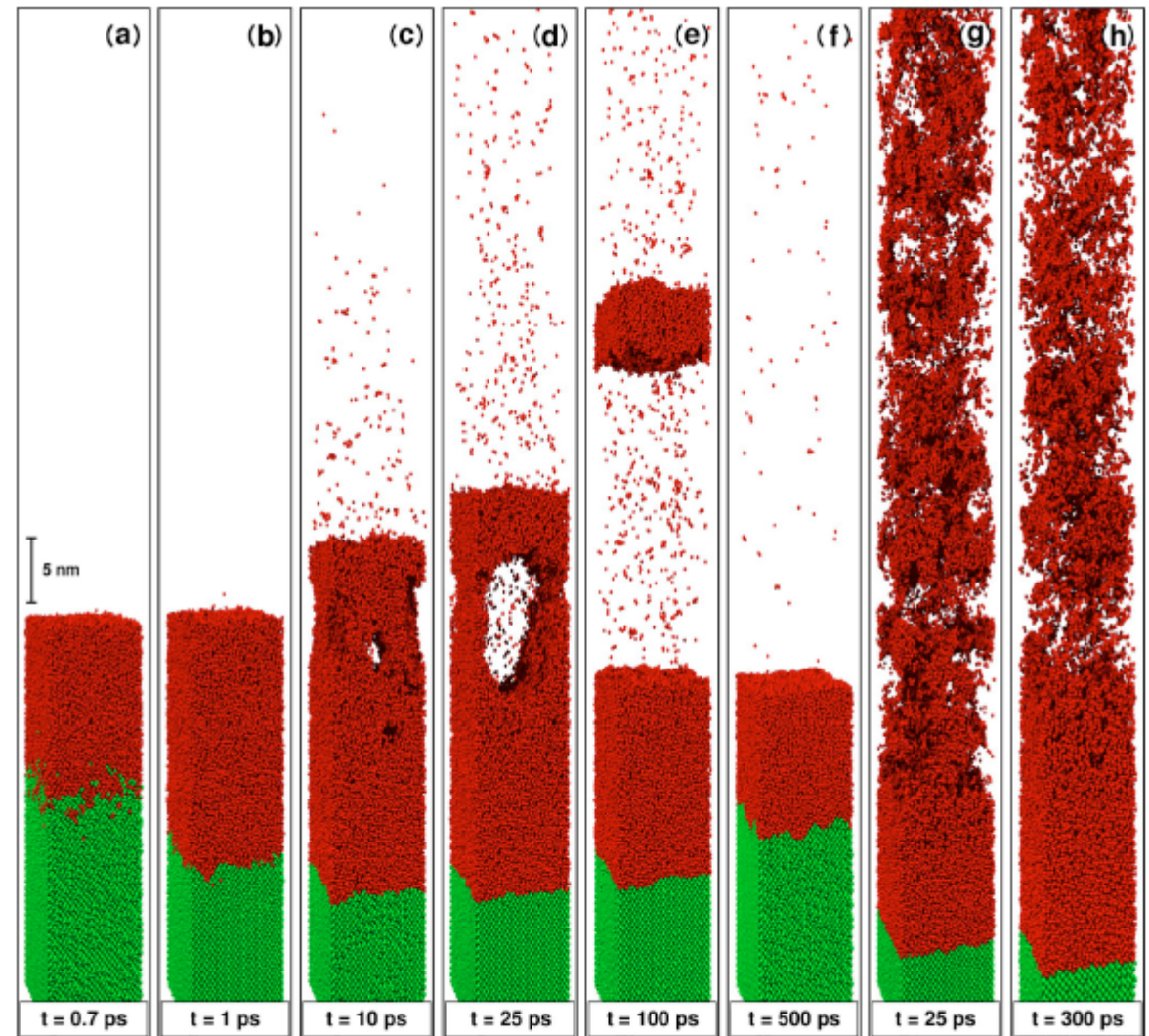


FIG. 4. (Color online) Snapshots revealing the structural changes induced in a Si(100) substrate by 500 fs and 100 ps pulses at 266 nm: (a)-(f) 500 fs pulse at a fluence $F = F_{in}^{fs} = 0.225\ J\ cm^{-2}$; (g) 500 fs pulse at a fluence $F = 2.2F_{in}^{fs} = 0.50\ J\ cm^{-2}$; (h) 100 ps pulse at a fluence $F = 1.1F_{in}^{ps} = 0.45\ J\ cm^{-2}$; F_{in}^{fs} and F_{in}^{ps} are the ablation thresholds under femtosecond and picosecond irradiation, respectively. Green: (semi-)conducting crystalline silicon; red: liquid silicon. Each pulse begins at $t = 0$.

XTRAM - in Ericc 28 July 2017

Bulk heating with FEL1

- Quasi-isotherm bulk heating can be obtained by using FEL1 pulses on several films (Al, Si, Ge, and more)
- Electron temperatures are estimated to be in the range 1-10 eV (WDM regime)
- Large-sized self-standing films are robust (0.1-0.3 microns thickness) and can be used for shot-to-shot experiments at the FEL repetition rate
- FEL2 useful for bulk heating of some important material (C for example)
- → **Soft x-ray FELs are really useful for efficient bulk heating!**

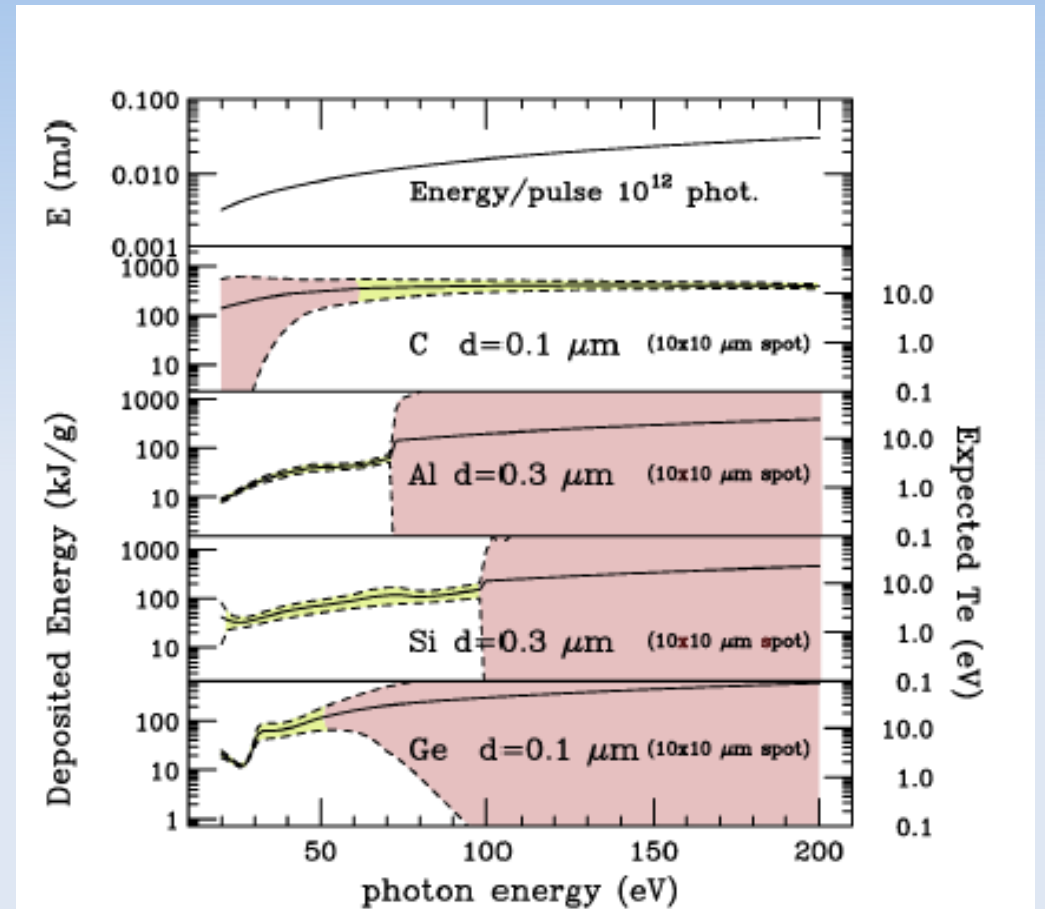
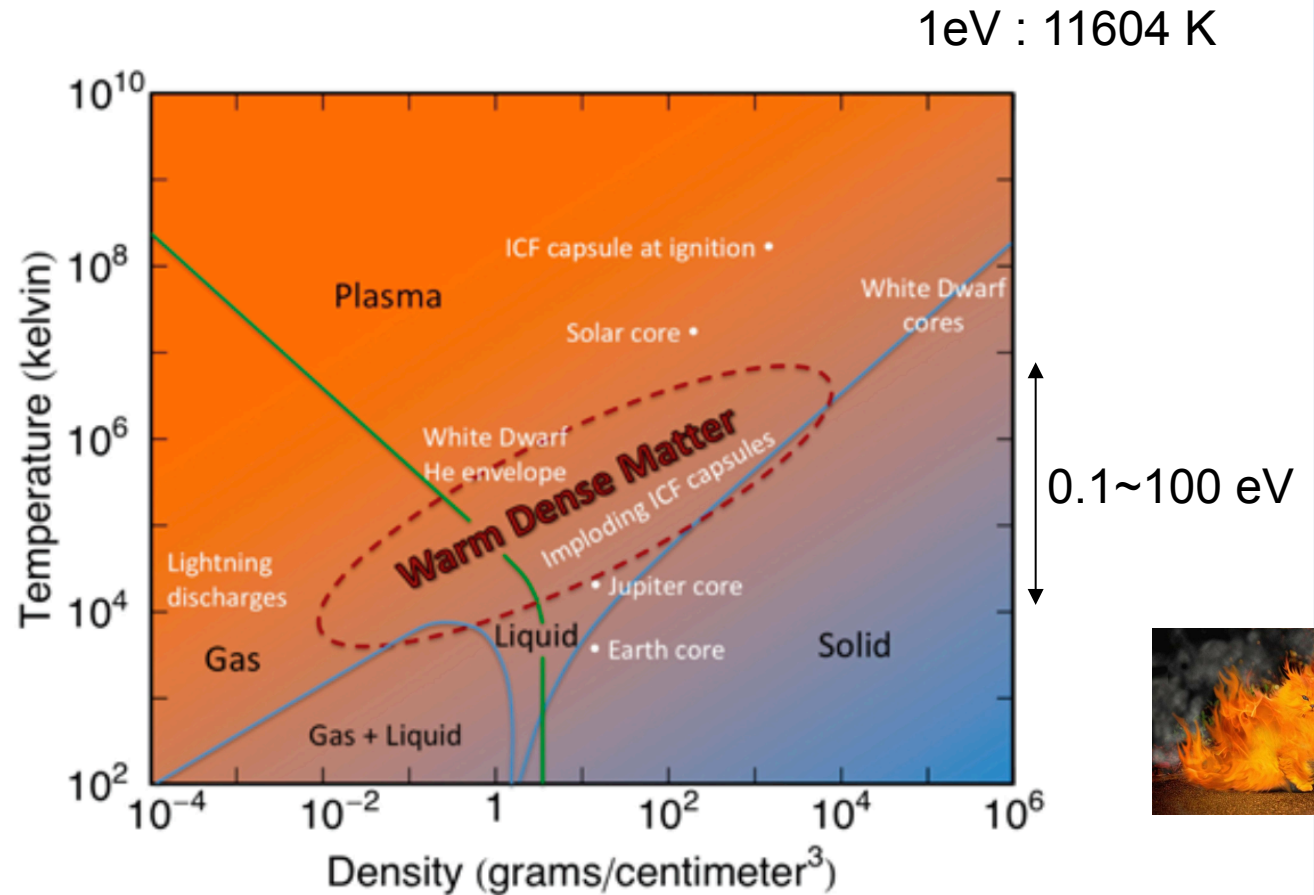
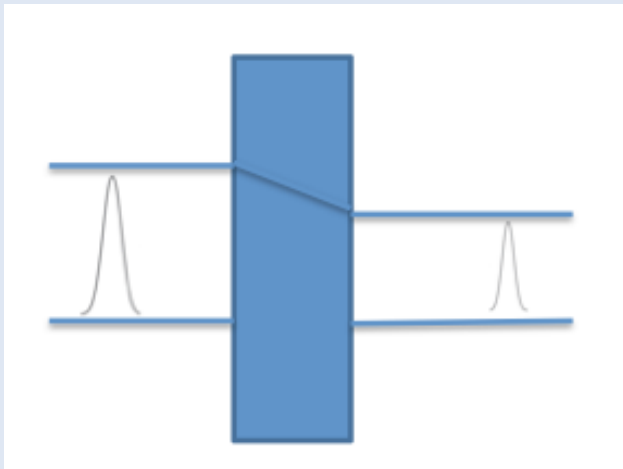


Figure 4. In the lower four panels we report the deposited energy (kJ per gram of substance) in different thin film materials as a function of the photon energy for a pulse containing 10^{12} photons (spot $10 \times 10 \mu\text{m}$). The deposited energy (solid curves) has been calculated accounting for possible saturation effects and show different trends according to the particular foil under consideration. The dashed curves represent the limits for the spread of deposited energy inside the films, so uniform bulk heating is obtained when the dashed curves define a narrow region (light green, color on-line). On the other hand, when most of the energy is deposited near the surface of the thin film, an extremely inhomogeneous heating is obtained (pink regions, color on-line). The expected electron temperature T_e is also shown on the right axis, showing that average temperatures in the 1-10 eV range are easily reached depending on the energy and thin foil material. The upper panel reports the pulse energy (mJ) as a function of the photon energy (eV) obviously changing of 1 order of magnitude from 20 to 200 eV. The FEL1 source (12-62 eV) turns out to be extremely efficient for obtaining uniform bulk heating of various materials (for example Al, Si, Ge shown in the picture).

Warm Dense Matter (WDM)

Application of VUV/X-FEL to solid. The pulse can heat the solid in ultra short time.

In saturation condition we can heat the material linearly



Temperature versus density for various structures in the universe. Pressures corresponding to this temperature and density are between 100,000 and one billion atmospheres. Figure from "Basic Research Needs for High Energy Density Laboratory Physics," DOE Office of Science and NNSA (2010).

Transmission at high fluence

- Saturable absorption in Al observed at FLASH (Nagler et al., Nat. Phys. 5, 693–696 (2009) with 92 eV photon energy (15 fs pulse width). Al $L_{2,3}$ -edges around 73 eV so the kinetic energy of photoelectron is about 20 eV. First TIMEX single-shot experiments at 23.7 eV (52.3 nm).

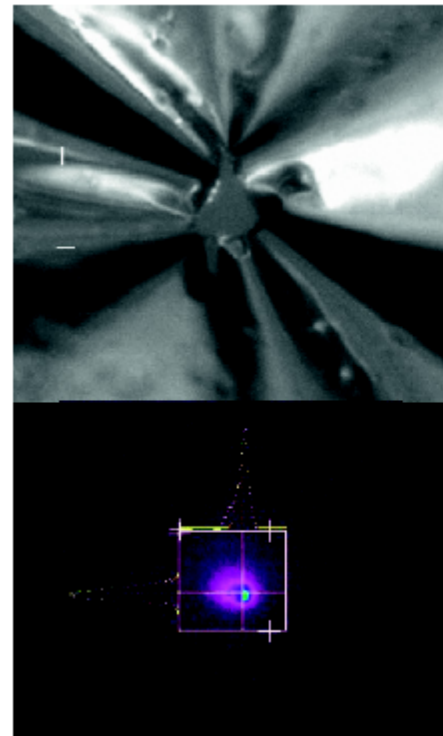
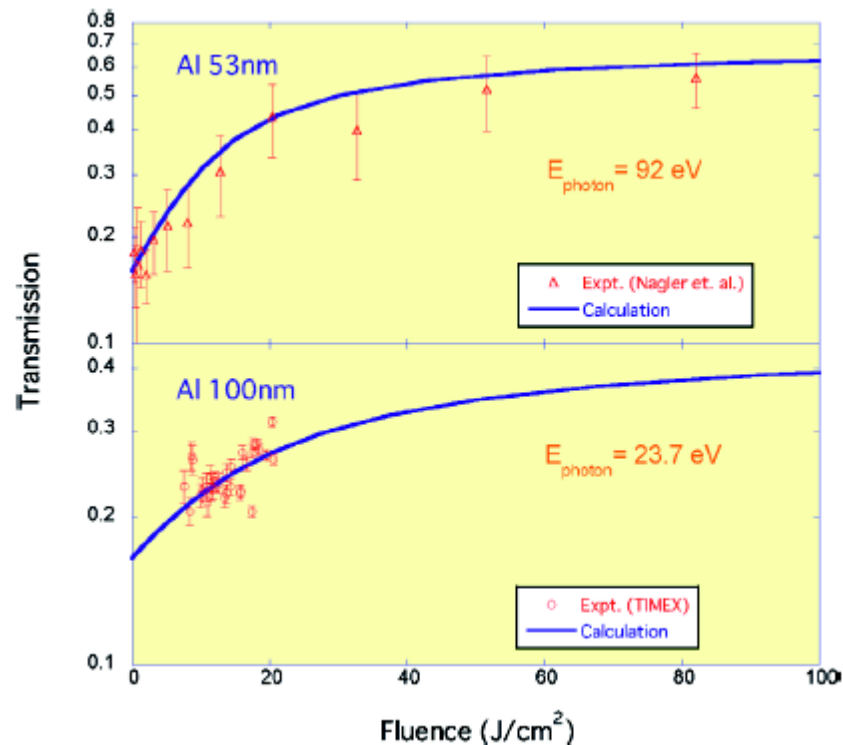


Figure 4

Left side: transmission of Al ultrathin foils as a function of the incident fluence of FEL pulses. The result of transmission measurements at the FLASH facility (see ref.⁷) and the first results obtained at TIMEX are compared with calculations (see text). Right side: the lower panel shows the lateral dimensions of the FEL pulses ($10 \times 10 \mu$ FWHM) at focus (as observed on a YAG screen by the TIMEX telemicroscope), the upper panel shows the effect of about 100 repeated FEL shots (fluence $10\text{--}20 \text{ J}/\text{cm}^2$) on a 100 nm ultrathin Al foil. The pulses of seed laser were not filtered and concur to the damage of the foil.

First measurement

nature
physics

ARTICLES

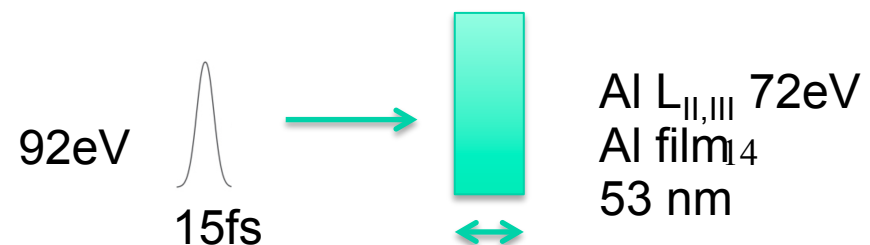
PUBLISHED ONLINE: 26 JULY 2009 | DOI: 10.1038/NPHYS1341

Turning solid aluminium transparent by intense soft X-ray photoionization

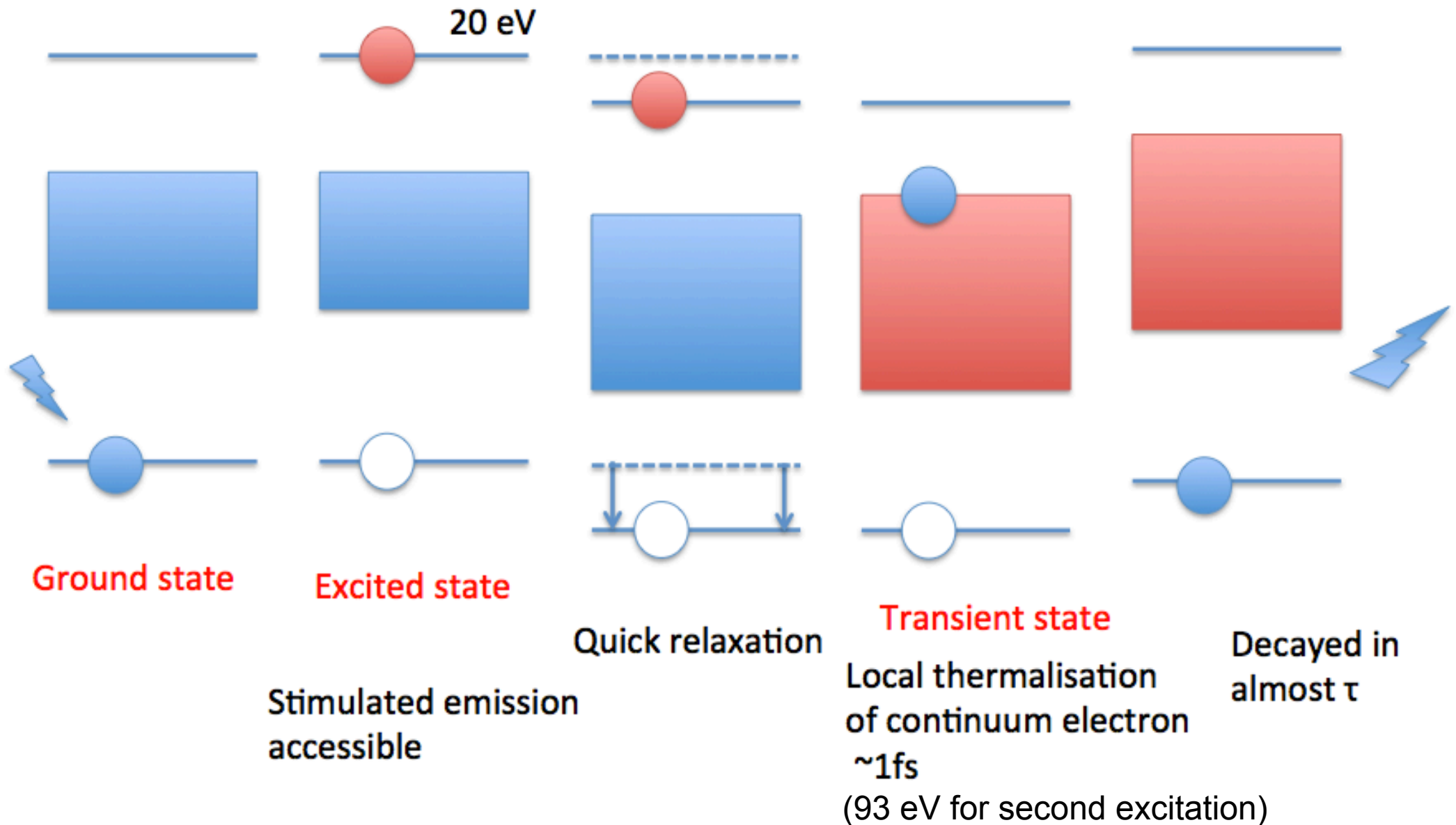
Bob Nagler et al.*

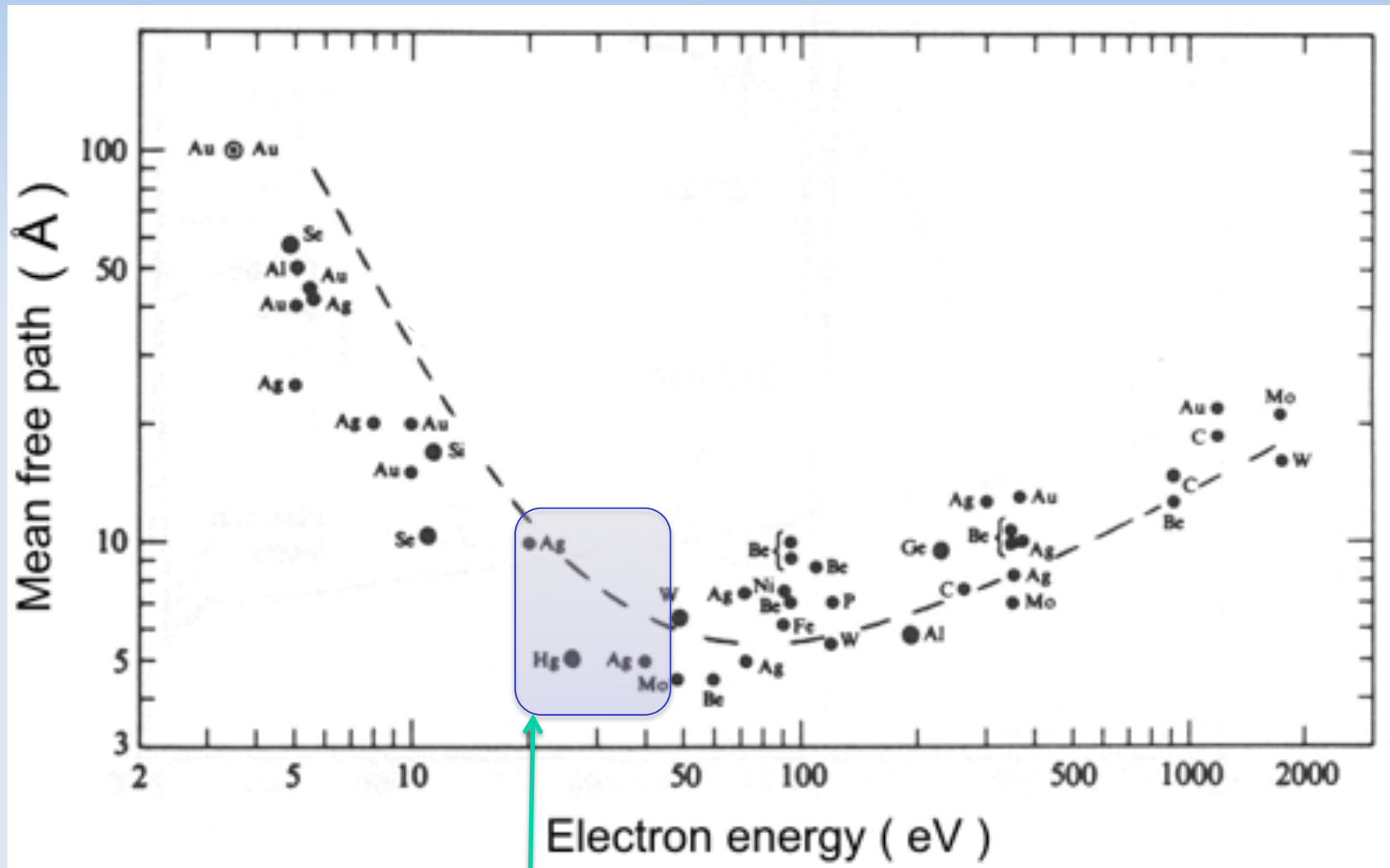
Saturable absorption is a phenomenon readily seen in the optical and infrared wavelengths. It has never been observed in core-electron transitions owing to the short lifetime of the excited states involved and the high intensities of the soft X-rays needed. We report saturable absorption of an L-shell transition in aluminium using record intensities over $10^{16} \text{ W cm}^{-2}$ at a photon energy of 92 eV. From a consideration of the relevant timescales, we infer that immediately after the X-rays have passed, the sample is in an exotic state where all of the aluminium atoms have an L-shell hole, and the valence band has approximately a 9 eV temperature, whereas the atoms are still on their crystallographic positions. Subsequently, Auger decay heats the material to the warm dense matter regime, at around 25 eV temperatures. The method is an ideal candidate to study homogeneous warm dense matter, highly relevant to planetary science, astrophysics and inertial confinement fusion.

FLASH Hamburg (2009)

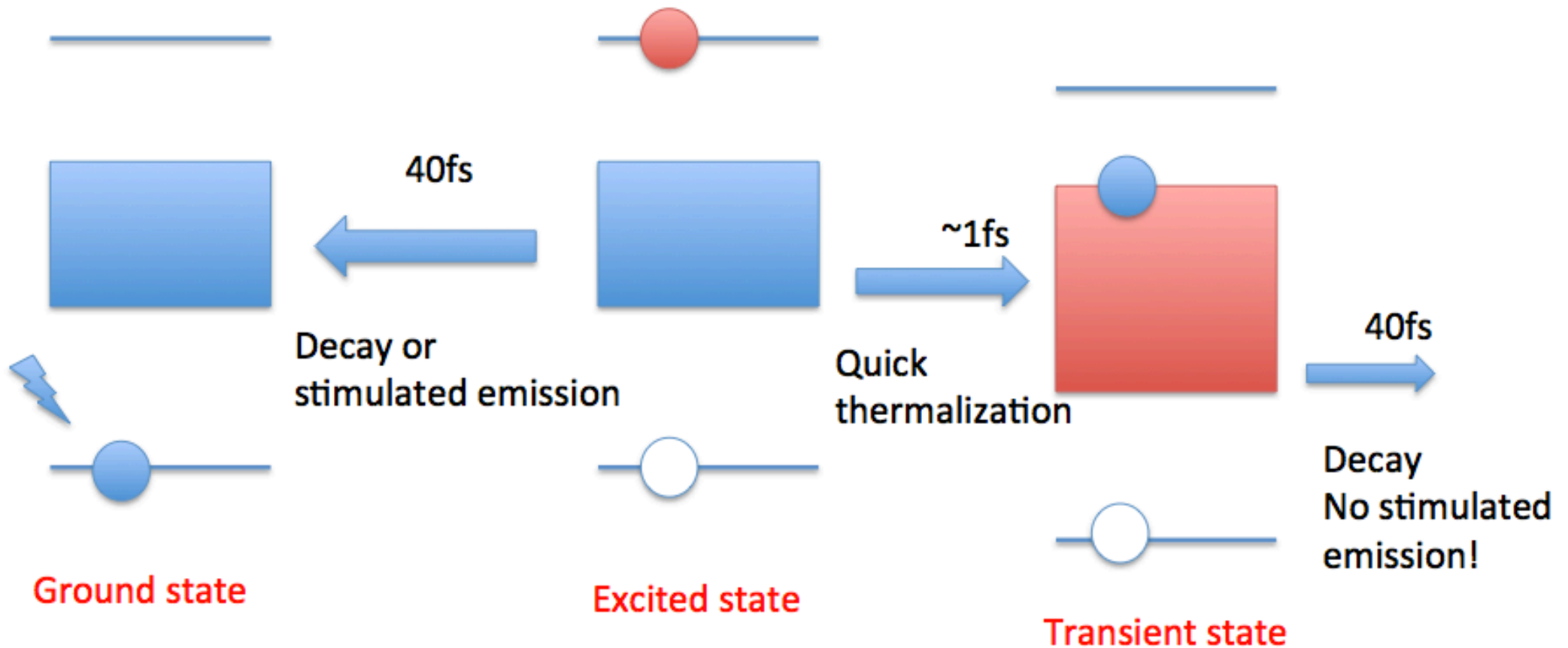


Simplification of the process





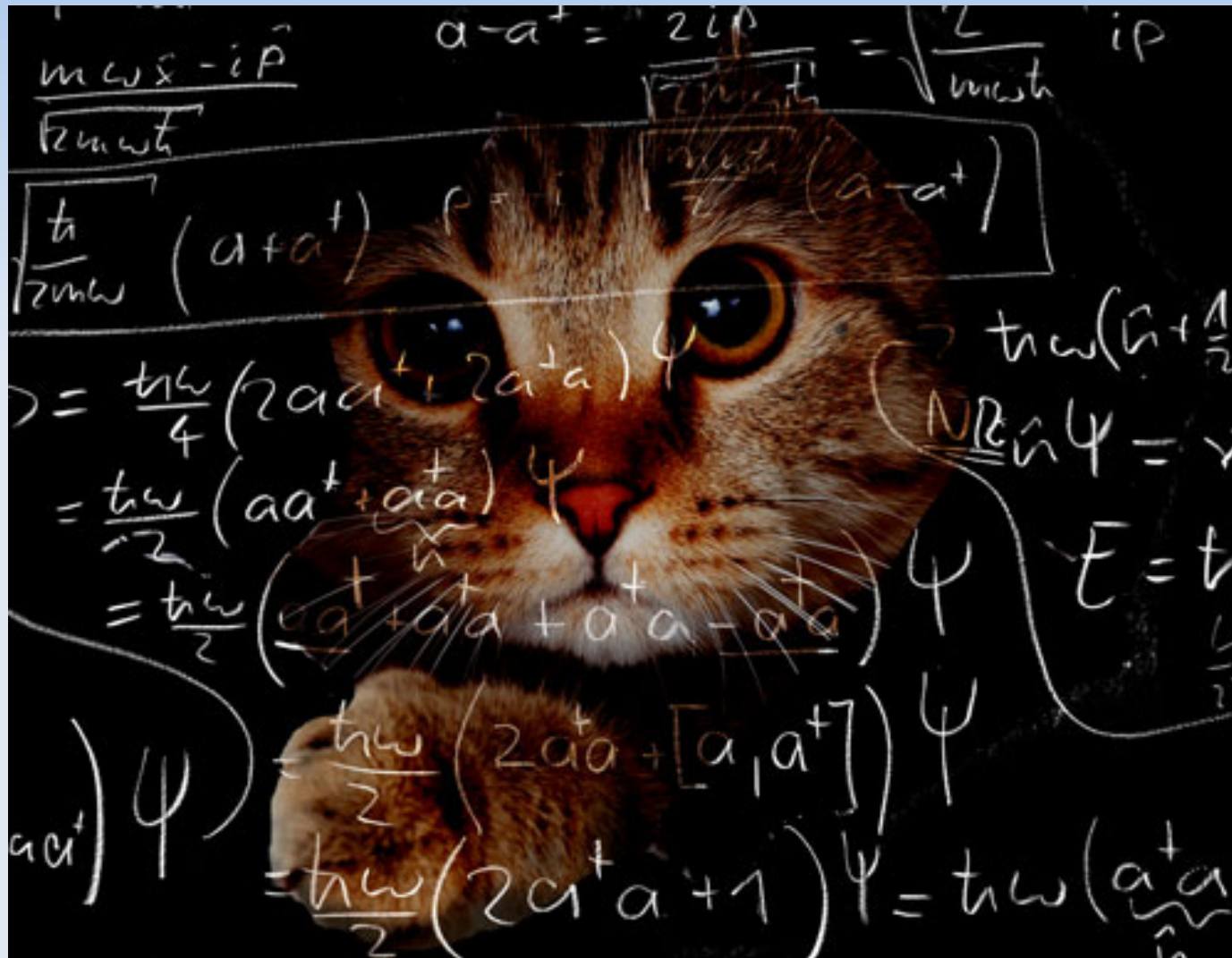
Three state model for core excitation



L-edge 72eV

93eV for second excitation

FORMULAS



Theoretical model

$$\frac{dN_1(z, t)}{dt} = \frac{a(z, t)I(z, t)}{\hbar\omega} + \frac{N_2(z, t)}{\tau_{21}} + \frac{N_3(z, t)}{\tau_{31}} \quad (1)$$

$$\frac{dN_2(z, t)}{dt} = -\frac{a(z, t)I(z, t)}{\hbar\omega} - \frac{N_2(z, t)}{\tau_{21}} - \frac{N_2(z, t)}{\tau_{23}} \quad (2)$$

$$\frac{dN_3(z, t)}{dt} = \frac{N_2(z, t)}{\tau_{23}} - \frac{N_3(z, t)}{\tau_{31}} \quad (3)$$

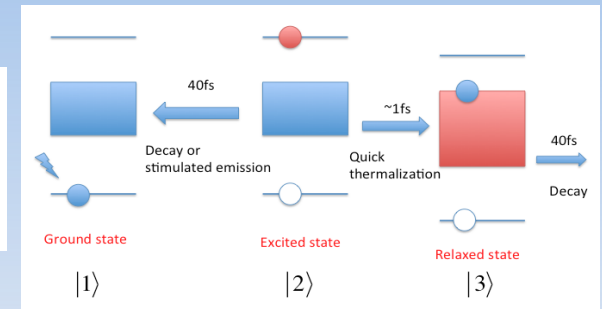
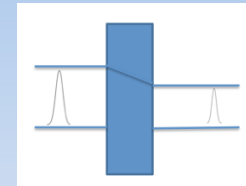
where

$$a(z, t) = \sigma \left(N_2(z, t) - \frac{d_2}{d_1} N_1(z, t) \right) \quad (4)$$

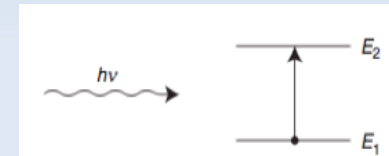
$$N = N_1(z, t) + N_2(z, t) + N_3(z, t) = \text{const.} \quad (5)$$

$a(z, t)$ is a generalized form of the absorption coefficient, for linear absorption process as Lambert-Beer, it must be a constant. The occupation numbers depend thus on the photon field intensity $I(z, t)$ at time t and position z , the photon absorption cross-section σ at given photon energy $\hbar\omega$, and on the relaxation times τ between the various states. d_2/d_1 is the degeneracy ratio of the states. These equations are coupled with the transport equation of the incoming laser pulse, within the classical electrodynamics limit:

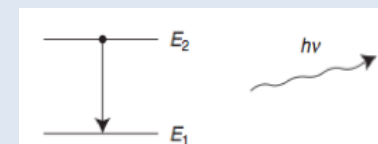
$$\frac{dI(z, t)}{dz} + \frac{1}{c} \frac{dI(z, t)}{dt} = a(z, t)I(z, t). \quad (6)$$



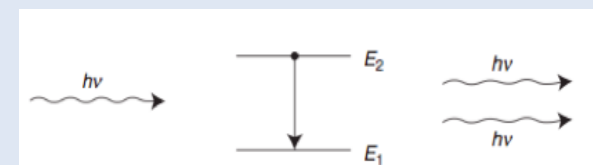
Absorption



Decay



Stimulated emission



Numerical code

where d_j is the degeneracy, or *statistical weight*, of level j . I have tried several numerical methods for this equations [1, 3], and at the end, what I have chosen was Upwind differencing method Eq. (20.1.27) in Ref [1], which is the simplest way to model the transport properties. The method is just employing the forward differenciation, as

$$\frac{I(z_j, t_{n+1}) - I(z_j, t_n)}{c\Delta t} = -\frac{I(z_j, t_n) - I(z_{j-1}, t_n)}{\Delta z} + g(z_j, t_n)I(z_j, t_n) \quad (3)$$

To reduce the error the step sizes should keep the following Courant condition,

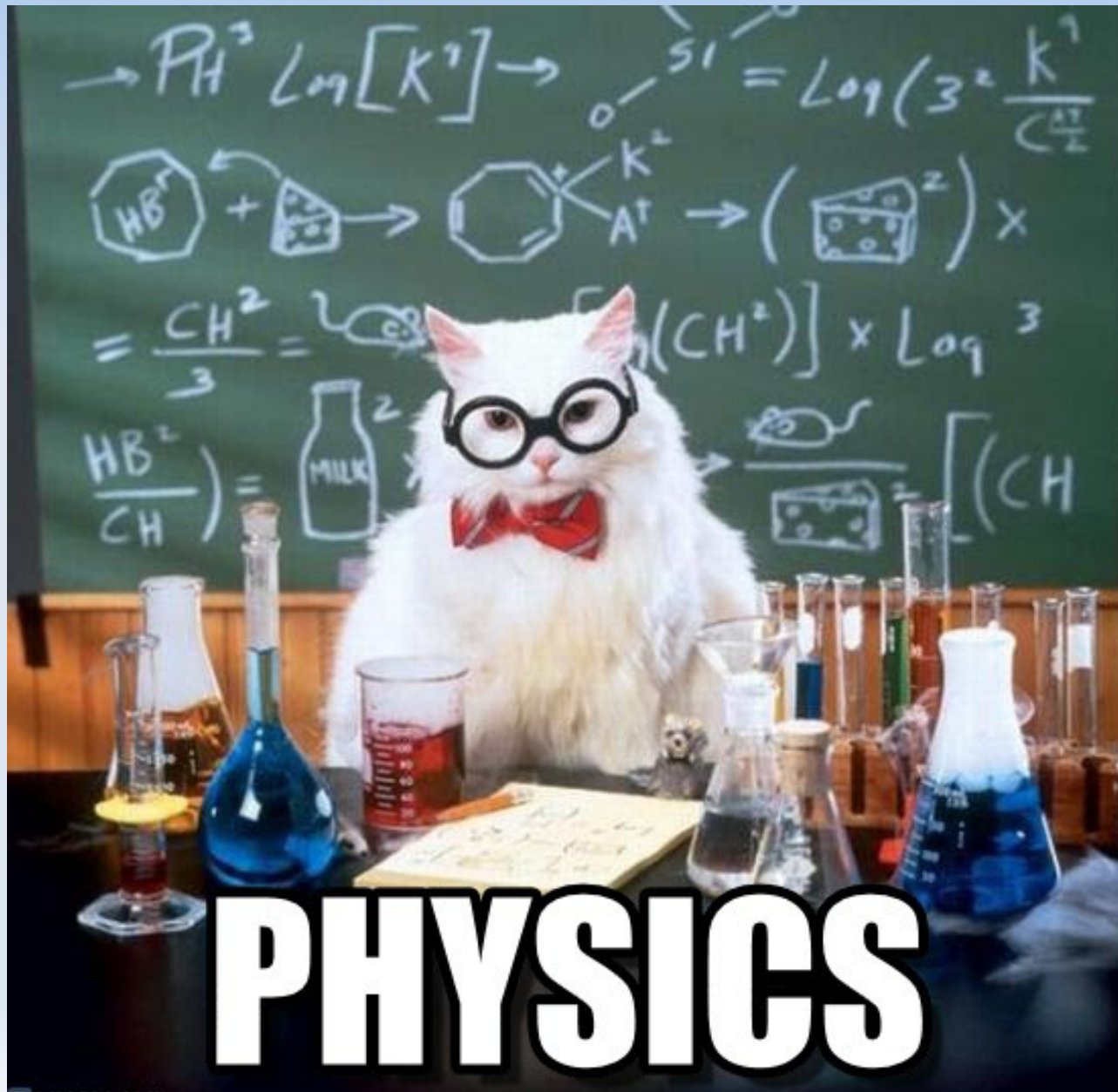
$$c \leq \frac{\Delta z}{\Delta t} \quad (4)$$

For the rate equation, I have just used *Euler* method, it is fine for our purpose,

$$\frac{N_2(z_j, t_{n+1}) - N_2(z_j, t_n)}{\Delta t} = -\frac{\sigma I(z_j, t_n)}{h\nu} \left[\left(1 + \frac{d_2}{d_1}\right) N_2(z_j, t_n) - \frac{d_2}{d_1} N \right] - \frac{N_2(z_j, t_n)}{\tau} \quad (5)$$

where I have used the relationship $N = N_1(z, t) + N_2(z, t) = \text{const.}$



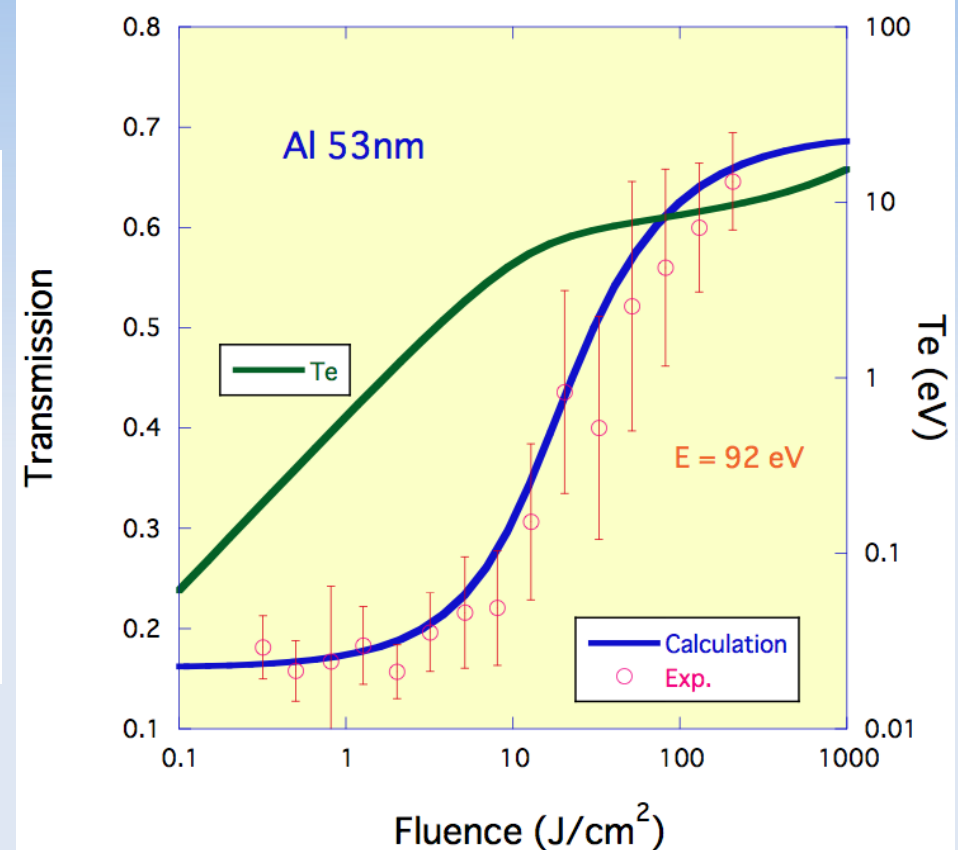
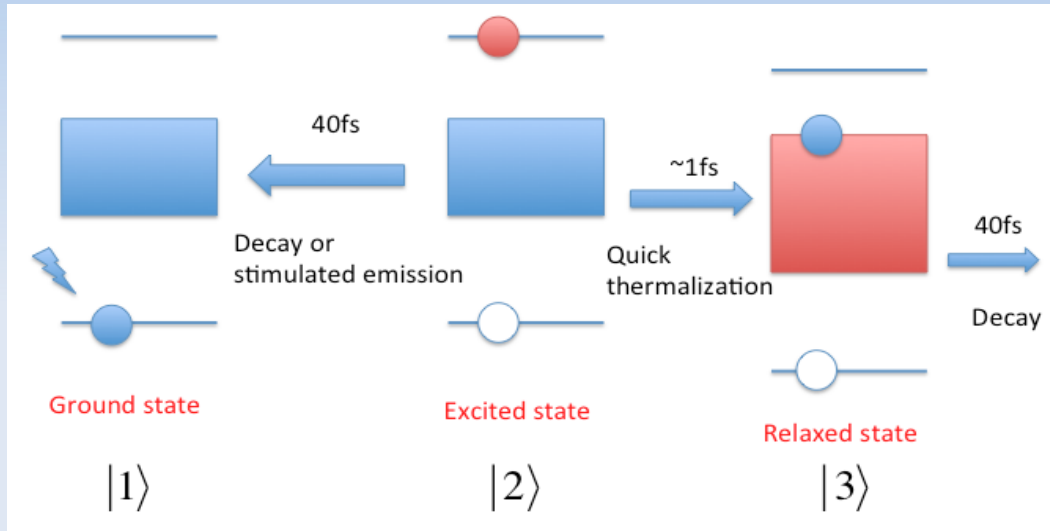


Comparison with calculations

Modeling saturable absorption for ultra short X-ray pulses

Keisuke Hatada^{a,b,*}, Andrea Di Cicco^a

Journal of Electron Spectroscopy and Related Phenomena xxx (2014)



$$\frac{dN_1(z, t)}{dt} = \frac{a(z, t)I(z, t)}{\hbar\omega} + \frac{N_2(z, t)}{\tau_{21}} + \frac{N_3(z, t)}{\tau_{31}} \quad (1)$$

$$\frac{dN_2(z, t)}{dt} = -\frac{a(z, t)I(z, t)}{\hbar\omega} - \frac{N_2(z, t)}{\tau_{21}} - \frac{N_2(z, t)}{\tau_{23}} \quad (2)$$

$$\frac{dN_3(z, t)}{dt} = \frac{N_2(z, t)}{\tau_{23}} - \frac{N_3(z, t)}{\tau_{31}} \quad (3)$$

where

$$a(z, t) = \sigma \left(N_2(z, t) - \frac{d_2}{d_1} N_1(z, t) \right) \quad (4)$$

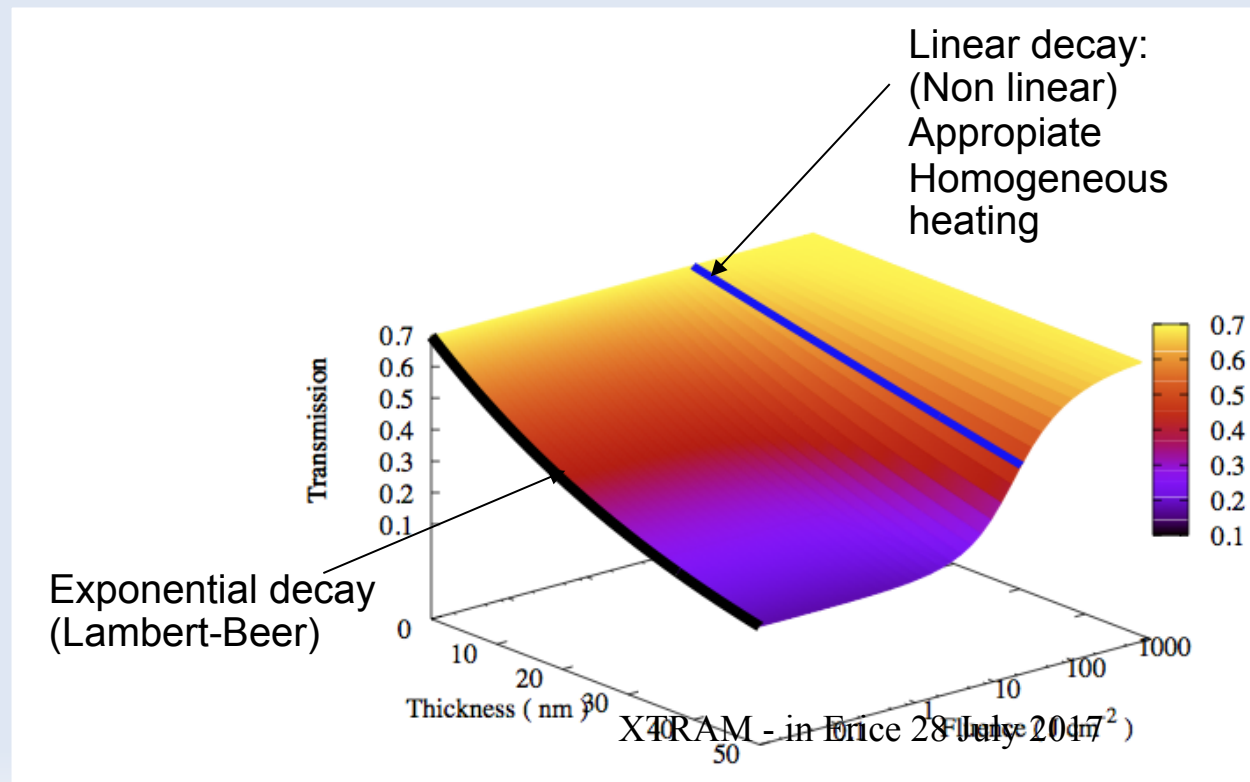
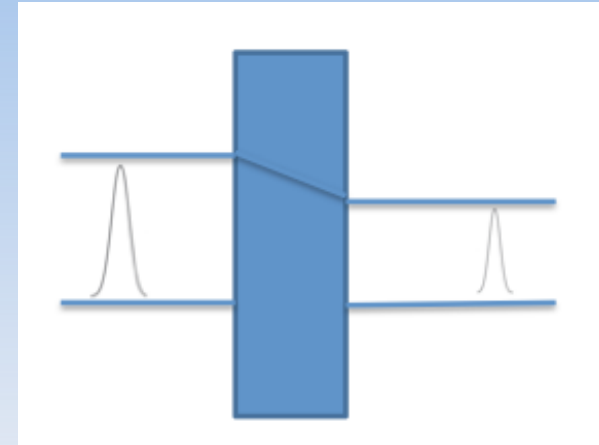
$$N = N_1(z, t) + N_2(z, t) + N_3(z, t) = \text{const.} \quad (5)$$

$$\frac{dI(z, t)}{dz} + \frac{1}{c} \frac{dI(z, t)}{dt} = a(z, t)I(z, t). \quad (6)$$

The photo-excited electrons have an energy of the order of 20 eV above the original Fermi energy. Measured inelastic scattering lengths for such electrons in aluminium are between 5 and 10 Å (ref. 21) corresponding to timescales of the order of 0.85–1.7 fs, in good agreement with calculations based on electron gas dielectric theory²². Thus, the photo-excited electrons rapidly lose their energy and thermalize with the initial cold valence electrons on a timescale considerably shorter than the FLASH pulse.

Observation of the attenuation with the fluence

- In the low fluence limit the attenuation is decreasing exponentially with the thickness (Lambert-Beer) while above the saturation threshold (about 1 J cm^2) linearly.



Long pulse steady state model

$$\frac{dN_1(z, t)}{dt} = \frac{dN_2(z, t)}{dt} = \frac{dN_3(z, t)}{dt} = 0, \quad \frac{dI(z, t)}{dt} = 0.$$

$$\frac{dI(z)}{dz} = \frac{g_0}{1 + \frac{I(z)}{\alpha I_s}} I(z)$$

$$g_0 = -\sigma(T)N$$

$$I_s = \frac{h\nu}{2\sigma\tau_{21}}$$

$$\alpha = 1 + \frac{2\tau_{21} - \tau_{31}}{2\tau_{23} + \tau_{31}}$$

$$I(z) = I_{sat} f_W^{-1} \left(\frac{I_0}{I_{sat}} e^{\frac{I_0}{I_{sat}}} e^{g_0 z} \right)$$

$$I_{sat} = \alpha I_s$$

Lambert Omega function

$$f_W(W) = We^W$$

For high fluence regime,

$$I \sim I_0 + I_{sat} g_0 z.$$

Theoretical model

~~$$\frac{dN_1(z, t)}{dt} = \frac{a(z, t)I(z, t)}{\hbar\omega} + \frac{N_2(z, t)}{\tau_{21}} + \frac{N_3(z, t)}{\tau_{31}} \quad (1)$$~~

~~$$\frac{dN_2(z, t)}{dt} = -\frac{a(z, t)I(z, t)}{\hbar\omega} - \frac{N_2(z, t)}{\tau_{21}} - \frac{N_2(z, t)}{\tau_{23}} \quad (2)$$~~

~~$$\frac{dN_3(z, t)}{dt} = \frac{N_2(z, t)}{\tau_{23}} - \frac{N_3(z, t)}{\tau_{31}} \quad (3)$$~~

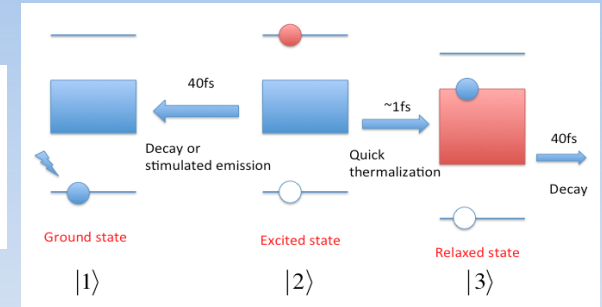
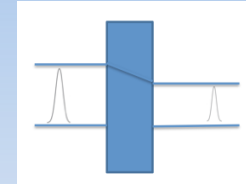
where

$$a(z, t) = \sigma \left(N_2(z, t) - \frac{d_2}{d_1} N_1(z, t) \right) \quad (4)$$

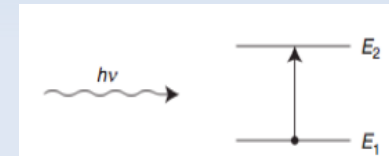
$$N = N_1(z, t) + N_2(z, t) + N_3(z, t) = \text{const.} \quad (5)$$

$a(z, t)$ is a generalized form of the absorption coefficient, for linear absorption process as Lambert-Beer, it must be a constant. The occupation numbers depend thus on the photon field intensity $I(z, t)$ at time t and position z , the photon absorption cross-section σ at given photon energy $\hbar\omega$, and on the relaxation times τ between the various states. d_2/d_1 is the degeneracy ratio of the states. These equations are coupled with the transport equation of the incoming laser pulse, within the classical electrodynamics limit:

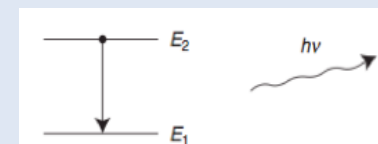
~~$$\frac{dI(z, t)}{dz} + \frac{1}{c} \frac{dI(z, t)}{dt} = a(z, t)I(z, t). \quad (6)$$~~



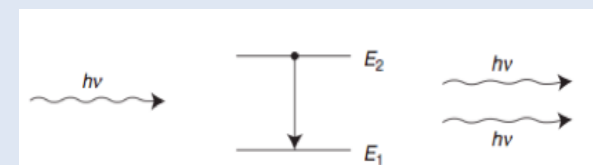
Absorption



Decay



Stimulated emission



Short pulse model

Frantz-Nodvik model:

Assuming the lifetimes are infinitely long, so that decaying part are dropped off

$$\phi(z) = \phi_{sat} \ln \left[1 + e^{g_0 z} \left(e^{\frac{\phi_0}{\phi_{sat}}} - 1 \right) \right]$$
$$\phi_{sat} = \frac{h\nu}{2\sigma}$$

Lifetimes are disappeared

For high fluence regime,

$$\phi(z) = \phi_0 + \phi_{sat} g_0 z.$$

Theoretical model

$$\frac{dN_1(z, t)}{dt} = \frac{a(z, t)I(z, t)}{\hbar\omega} + \frac{N_2(z, t)}{\tau_{21}} + \frac{N_3(z, t)}{\tau_{31}} \quad (1)$$

$$\frac{dN_2(z, t)}{dt} = -\frac{a(z, t)I(z, t)}{\hbar\omega} - \frac{N_2(z, t)}{\tau_{21}} - \frac{N_2(z, t)}{\tau_{23}} \quad (2)$$

$$\frac{dN_3(z, t)}{dt} = \frac{N_2(z, t)}{\tau_{23}} - \frac{N_3(z, t)}{\tau_{31}} \quad (3)$$

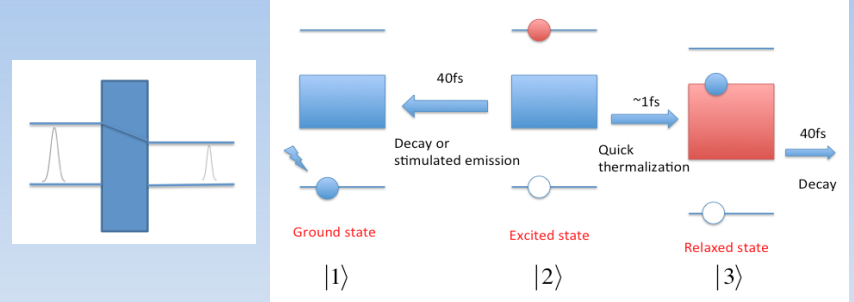
where

$$a(z, t) = \sigma \left(N_2(z, t) - \frac{d_2}{d_1} N_1(z, t) \right) \quad (4)$$

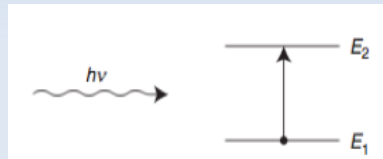
$$N = N_1(z, t) + N_2(z, t) + N_3(z, t) = \text{const.} \quad (5)$$

$a(z, t)$ is a generalized form of the absorption coefficient, for linear absorption process as Lambert-Beer, it must be a constant. The occupation numbers depend thus on the photon field intensity $I(z, t)$ at time t and position z , the photon absorption cross-section σ at given photon energy $\hbar\omega$, and on the relaxation times τ between the various states. d_2/d_1 is the degeneracy ratio of the states. These equations are coupled with the transport equation of the incoming laser pulse, within the classical electrodynamics limit:

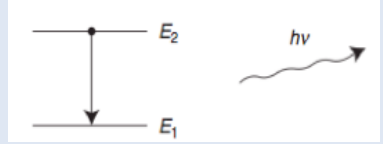
$$\frac{dI(z, t)}{dz} + \frac{1}{c} \frac{dI(z, t)}{dt} = a(z, t)I(z, t). \quad (6)$$



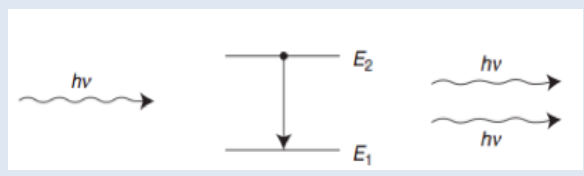
Absorption



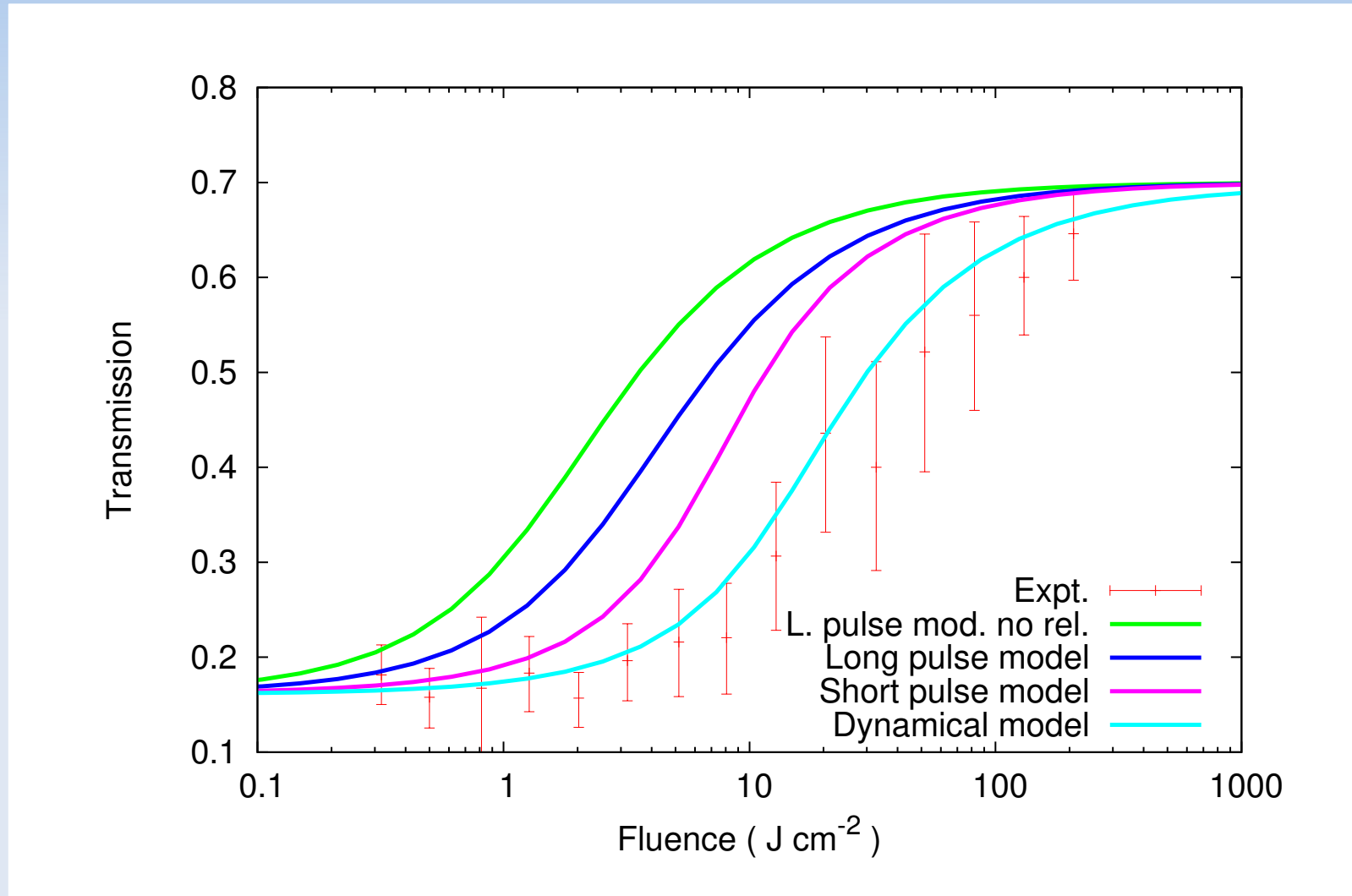
Decay



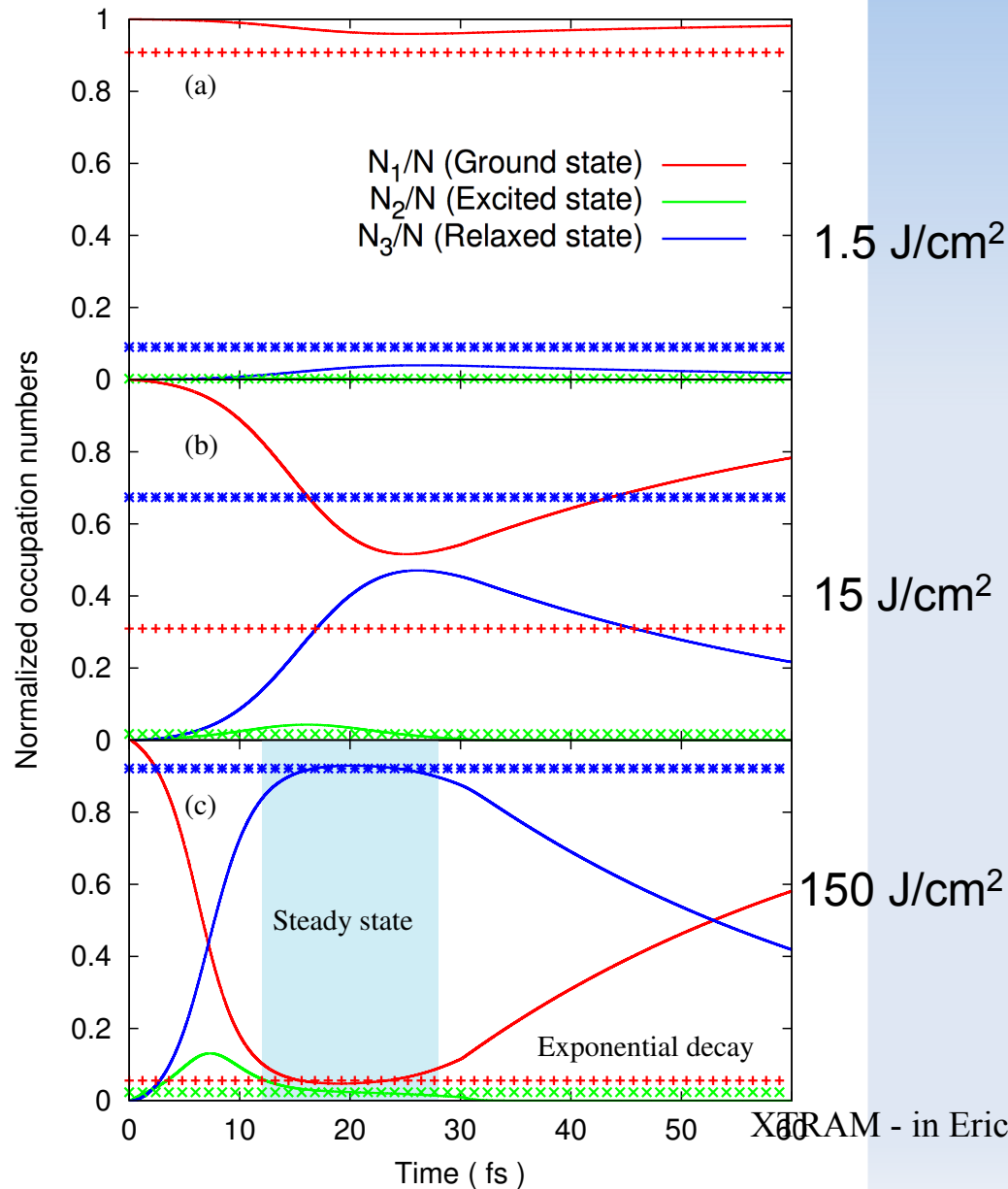
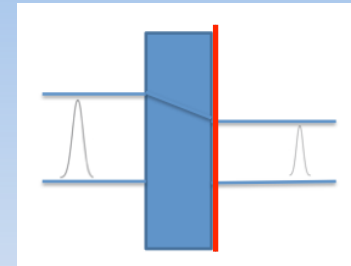
Stimulated emission



Comparison with steady state approximations



Dynamics at the end surface



Time dependence of the density of occupation numbers (normalized by the total number N) at the end face of Al thin film. The solid curves and dotted lines are estimated by the three channel model and Long pulse model, respectively. After some time, the curves asymptotically approaches to the steady state of Long pulse model. In the region of the light blue shade, the system has reached a steady state. After about 30 fs which is the total pulse width, the excited state decays exponentially. The averaged experimental data are indicated by red points with the errors.

Two Photon Absorption (TPA)

$$\frac{dN_1(z,t)}{dt} = \frac{g(z,t)I(z,t)}{h\nu} + \frac{g_2(z,t)I^2(z,t)}{h\nu} + \frac{N_2(z,t)}{\tau_{21}} + \frac{N_T(z,t)}{\tau_{T1}}$$

$$\frac{dN_2(z,t)}{dt} = -\frac{g(z,t)I(z,t)}{h\nu} - \frac{N_2(z,t)}{\tau_{21}}$$

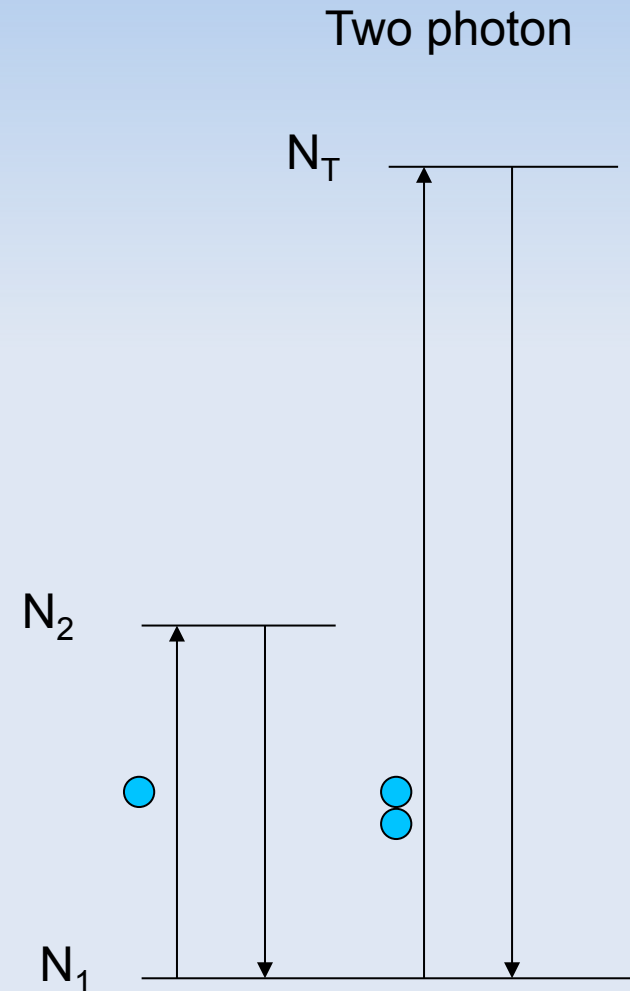
$$\frac{dN_T(z,t)}{dt} = -\frac{g_2(z,t)I^2(z,t)}{h\nu} - \frac{1}{\tau_{T1}}N_T(z,t)$$

$$\frac{dI(z,t)}{dz} + \frac{1}{c} \frac{dI(z,t)}{dt} = g(z,t)I(z,t) + g_2(z,t)I^2(z,t)$$

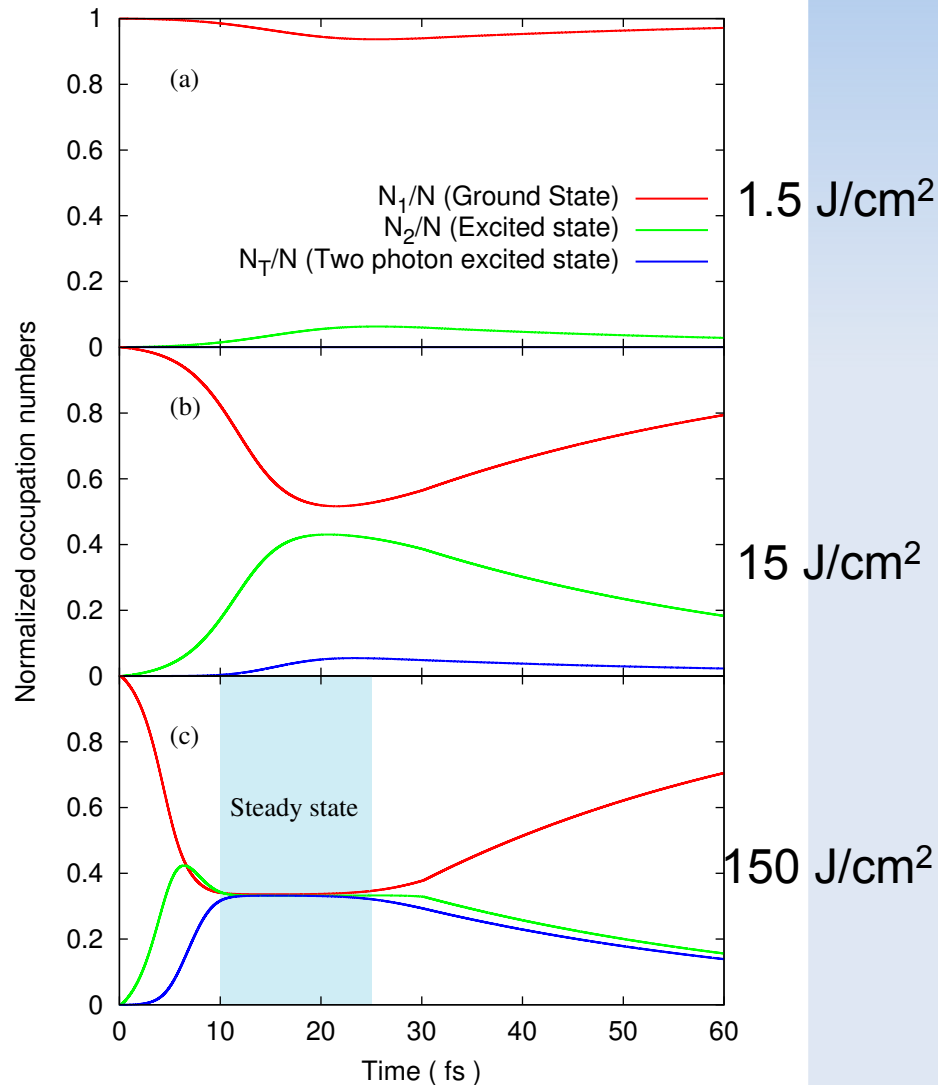
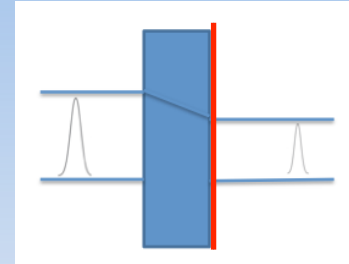
$$g(z,t) = \sigma (N_2(z,t) - N_1(z,t))$$

$$g_2(z,t) = \frac{\sigma_2}{h\nu} (N_T(z,t) - N_1(z,t))$$

$$N = N_1(z,t) + N_2(z,t) + N_T(z,t)$$

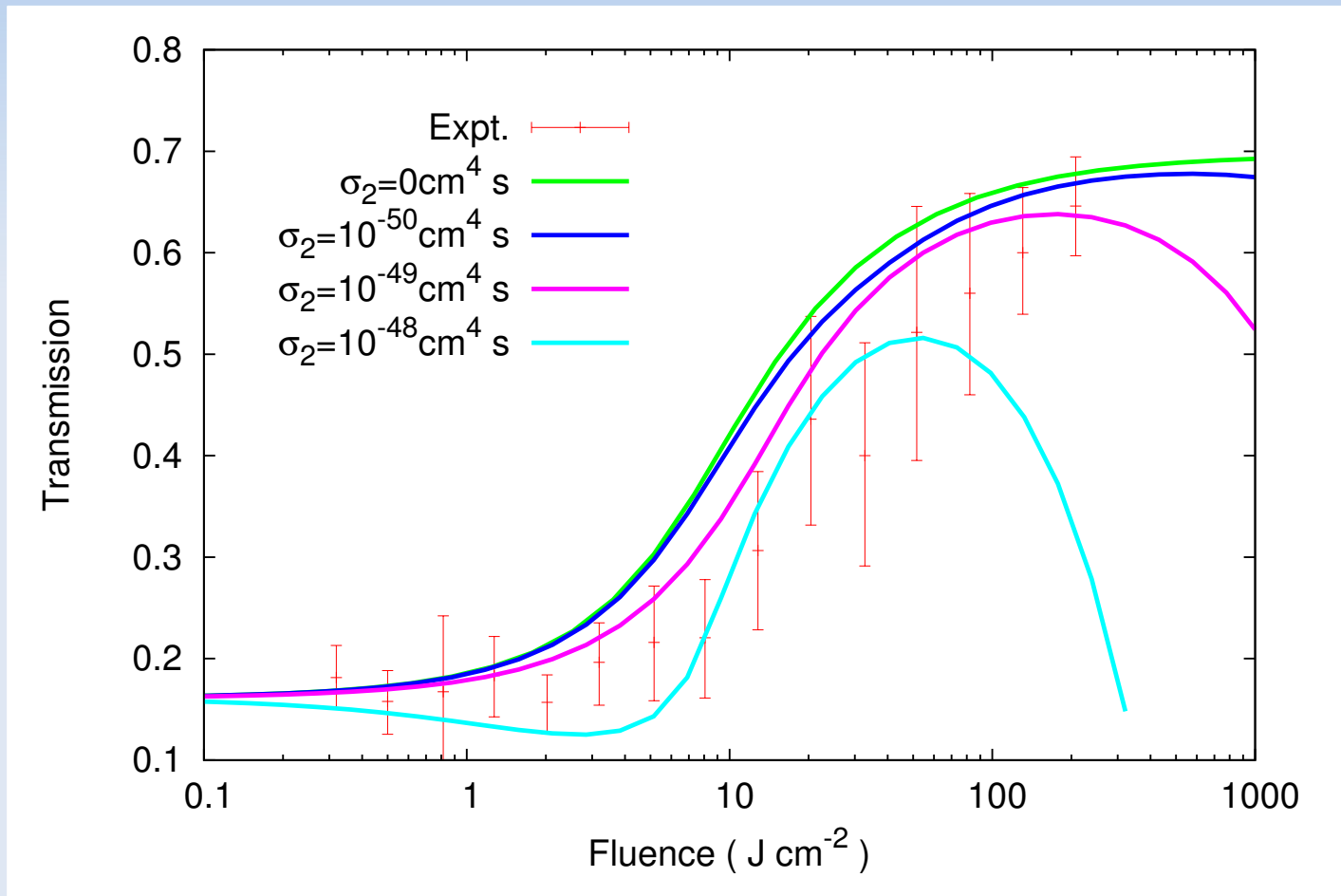


Two Photon Absorption (TPA)

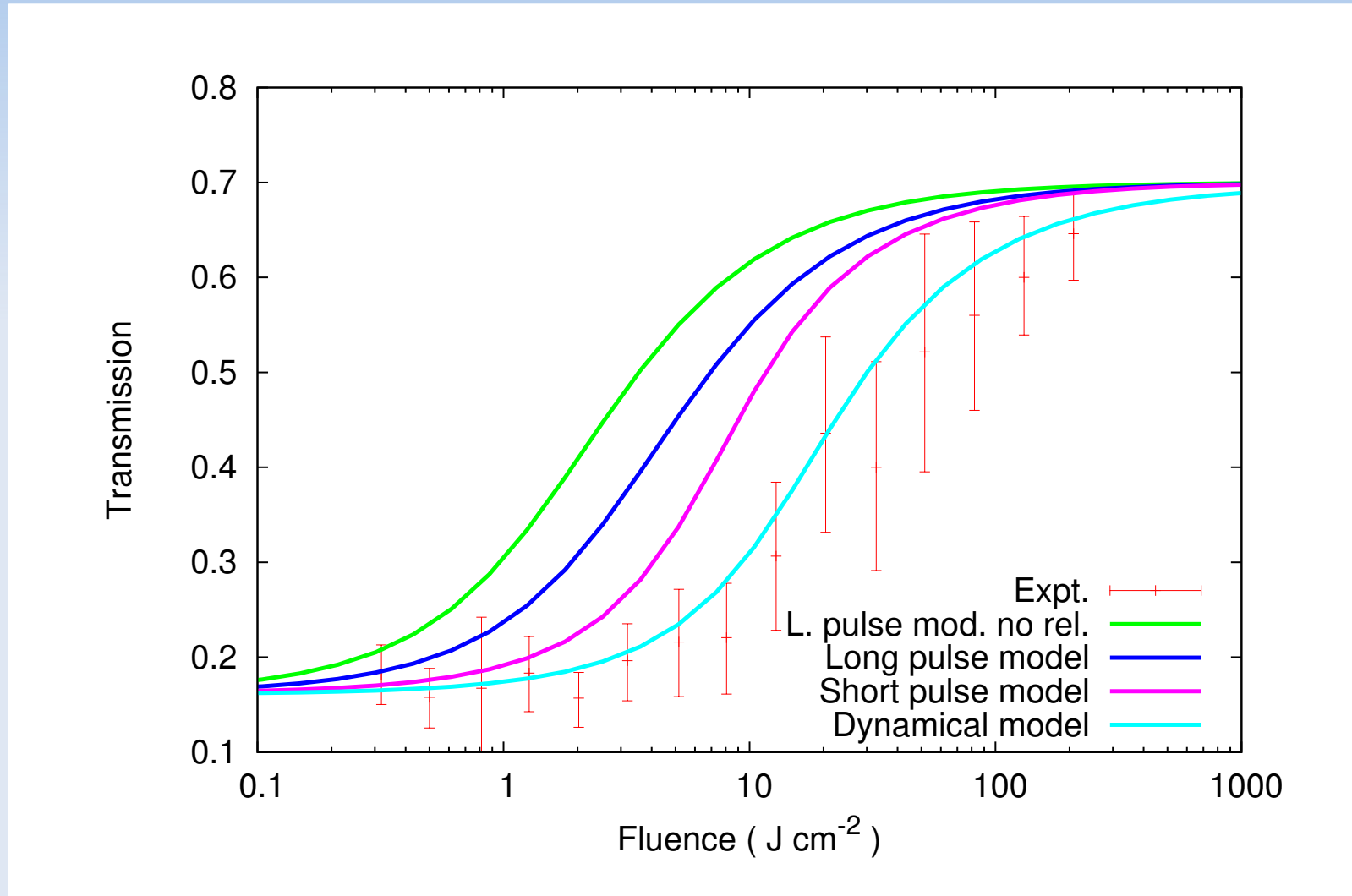


Time dependence of the density of occupation numbers (normalized by the total number N) at the end surface of the Al thin film (53nm), using the two-photon absorption (TPA) contribution at 92 eV photon energy (FEL pulse). The TPA cross section σ^2 is set to $10^{-50}\text{cm}^4\text{s}$.

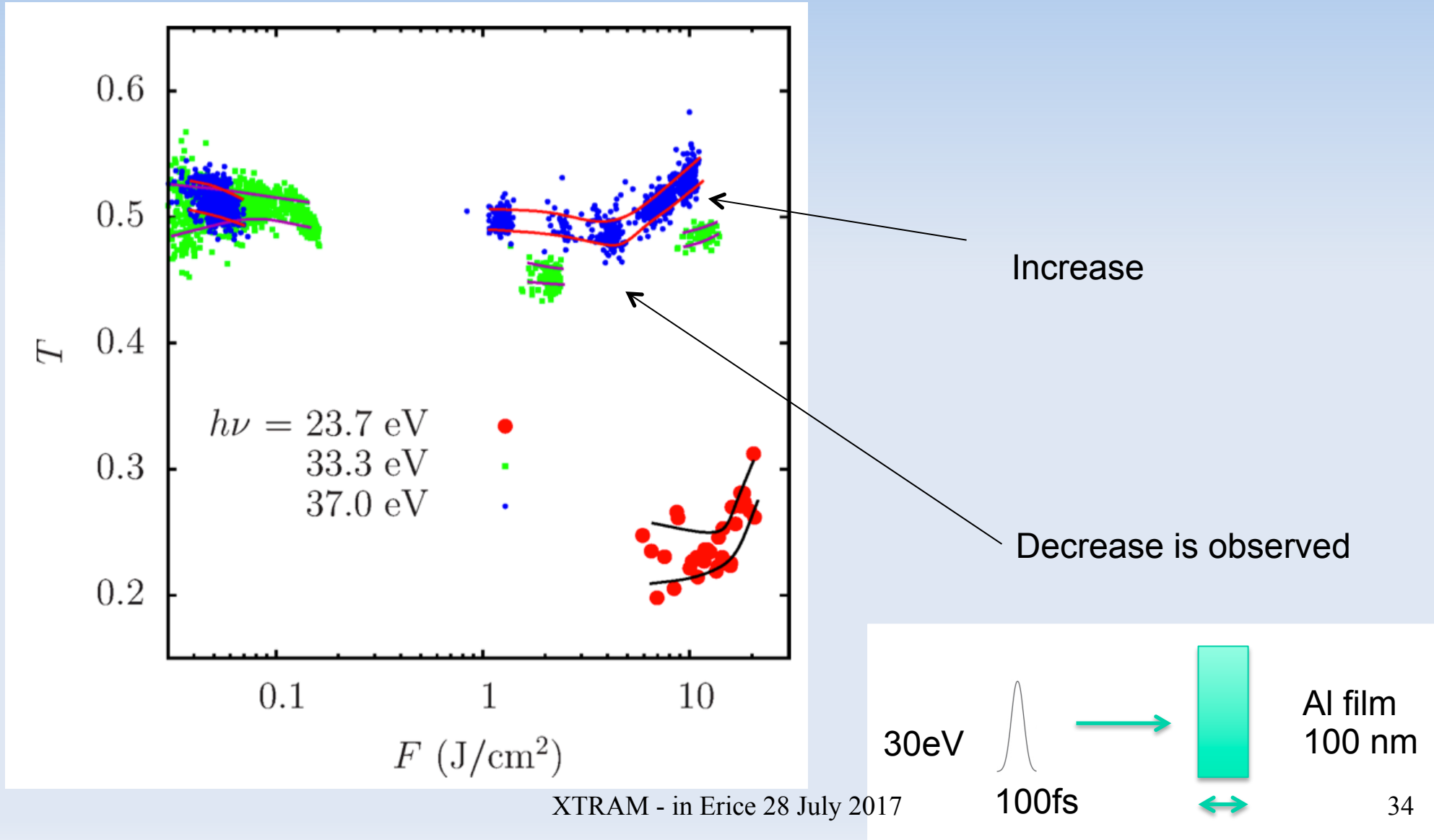
Saturation by TPA



Comparison with steady state approximations



TIMEX experiment



Nonlinear absorption of Al thin-film by EUV-FEL

High Energy Density Physics 5 (2009) 124–131

Free-free opacity in warm dense aluminum

Sam M. Vinko^{a,*}, Gianluca Gregori^a, Michael P. Desjarlais^b, Bob Nagler^a, Thomas J. Whitcher^a, Richard W. Lee^c, Patrick Audebert^d, Justin S. Wark^a

- Calculations (photon energy 30 eV) shows an increased opacity under different conditions while saturation effects start above 20 J/cm²

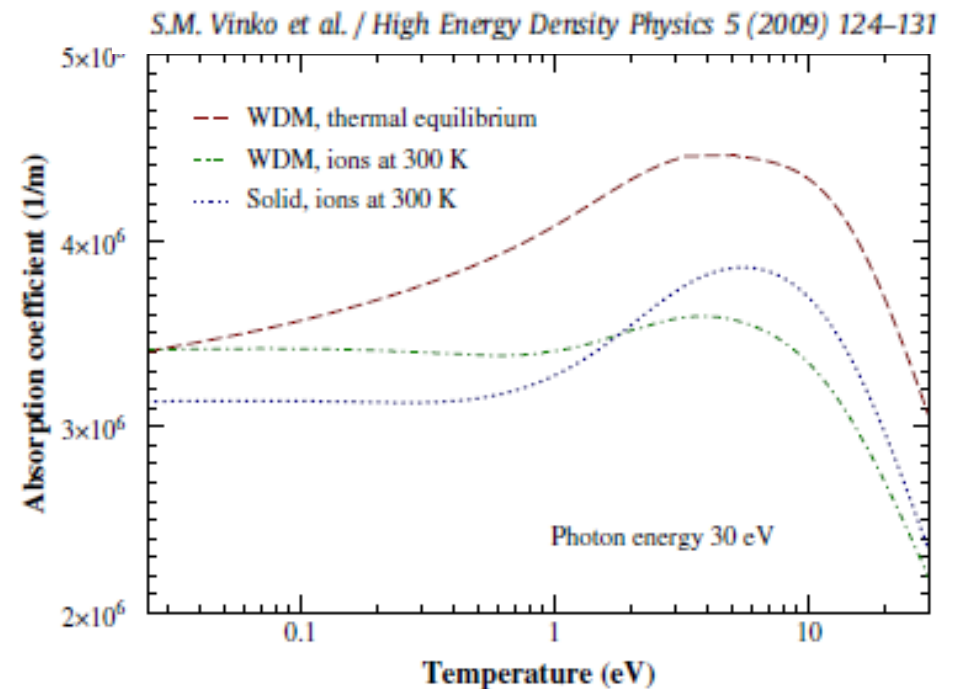


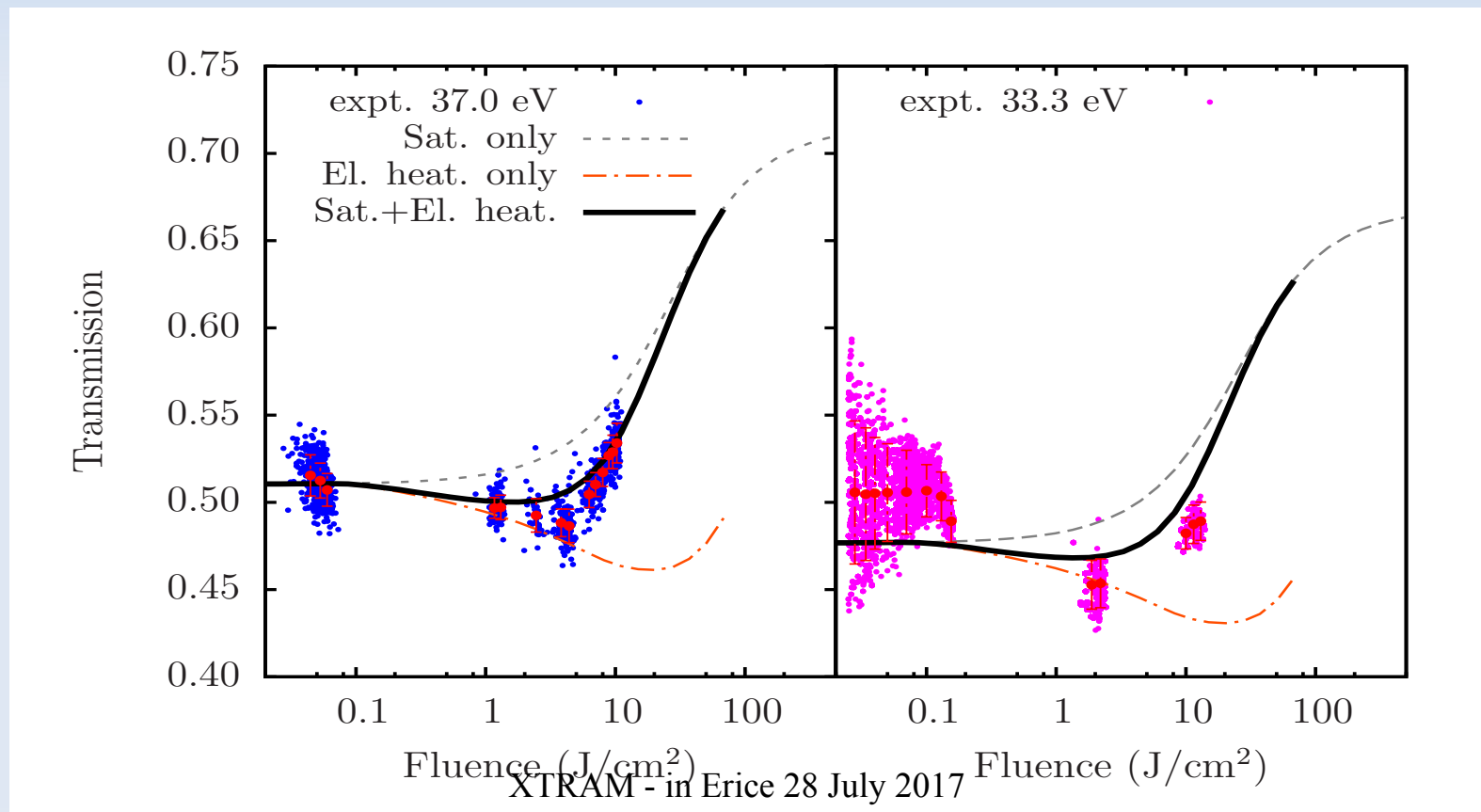
Fig. 8. Absorption coefficient versus temperature for warm dense Al in thermal equilibrium (red), warm dense Al with ions at room temperature (green) and solid Al with ions at room temperature (blue). Solid density and constant ionization $Z=3$.

Combining optical saturation and temperature effect for EUV

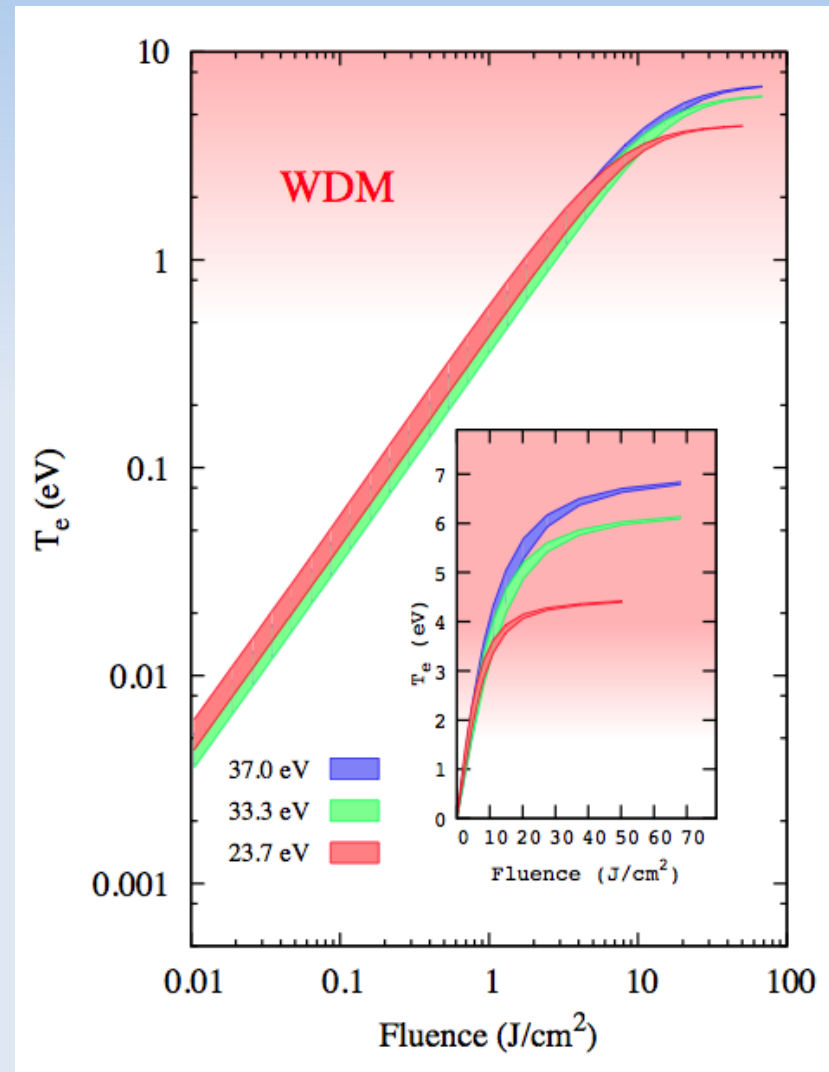
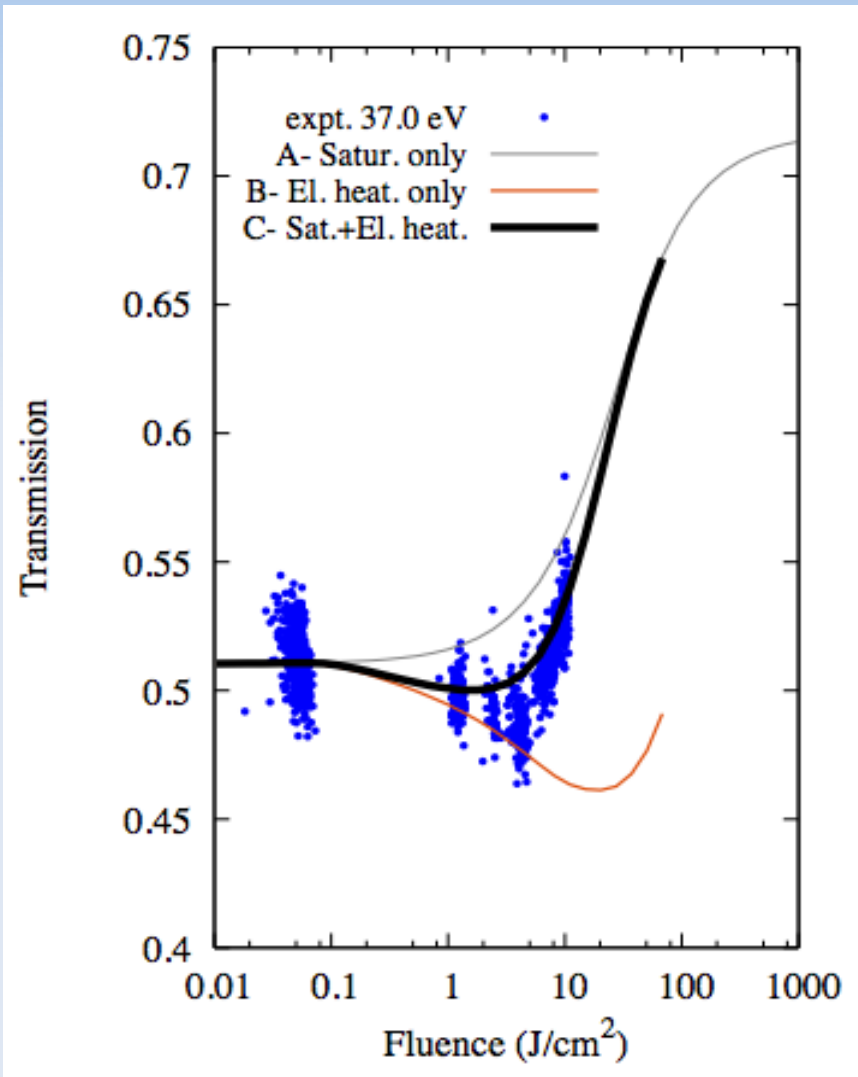
Another experimental run performed at 37.3 nm and 33 nm (33.5 and 37.5 eV) with improved collection strategies

Observation of a slightly decreased transmittance (10%) at intermediate fluence (1-2 J/cm²), followed by a rise up to 10-20 J/cm².

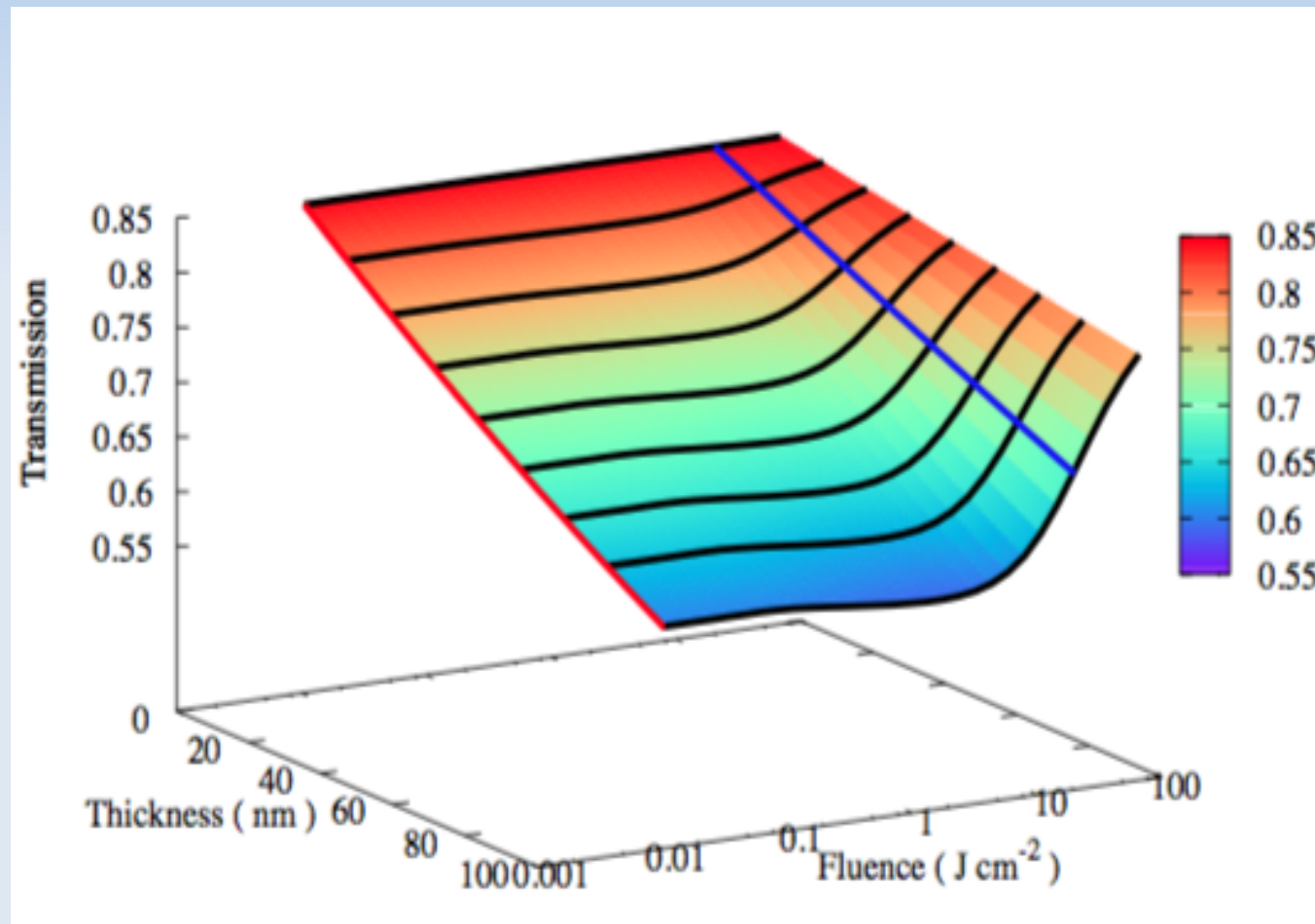
Calculations reproduced both features decrease (due to temperature) and increase (due to saturation) opacities



Combining optical saturation and temperature effect for EUV



Transmission with thickness and fluence



END of Talk

Thank you for your attention!

More infos can be found in ...

RAPID COMMUNICATIONS

PHYSICAL REVIEW B **90**, 220303(R) (2014)

Interplay of electron heating and saturable absorption in ultrafast extreme ultraviolet transmission of condensed matter

Andrea Di Cicco,¹ Keisuke Hatada,^{2,1} Erika Giangrisostomi,³ Roberto Gunnella,¹ Filippo Bencivenga,³ Emiliano Principi,³ Claudio Masciovecchio,³ and Adriano Filippini⁴

Journal of Electron Spectroscopy and Related Phenomena 196 (2014) 177-180

Modeling saturable absorption for ultra short X-ray pulses

Keisuke Hatada^{a,b,*}, Andrea Di Cicco^a

Research Infrastructures

Probing matter under extreme conditions at the free-electron-laser facilities: the TIMEX beamline

ANDREA DI CICCOC, CLAUDIO MASCOVECCHIO^b, FILIPPO BENCIVENGA^b, EMILIANO PRINCIPI^b, ERIKA GIANGRISOSTOMI^b, ANDREA BATTISTONI^b, RICCARDO CUCINI^b, FRANCESCO D'AMICO^b, SILVIA DI FONZO^b, ALESSANDRO GESSINI^b, KEISUKE HATADA^a, ROBERTO GUNNELLA^a, ADRIANO FILIPPINI^c


^aCNISM, Sezione di Fisica, Scuola di Scienze e Tecnologie, Università di Camerino, via Madonna delle Carceri 9, I-62032 Camerino (MC), Italy.

^bSynchrotron ELETTRA, Strada Statale 14 - I-34149 Basovizza, Trieste, Italy.

^cDipartimento di Scienze Fisiche e Chimiche, Università degli Studi dell'Aquila, I-67100 L'Aquila, Italy

XTRAM - in Erice 28 July 2017

Notiziario Neutroni e Luce di Sincrotrone Volume 18 n. 2



TIMEX

an end-station for ultrafast Time-resolved studies of Matter under EXtreme and metastable conditions

[Home](#) [Contacts](#) [Links](#) [Sharing and](#)

NEWS

- December 20, 2011
The TIMEX elliptic focusing mirror was not delivered on schedule for RUN 9 and the DIPROI end-station has been used for TIMEX experiments.
- December 21-22, 2011
We succeeded in scanning the M_{4,5} absorption edge (about 29.5 eV) of Ge by exploiting the tuning capabilities of FERMI (RUN 9). The TIMEX campaign of measurements was carried out in transmission geometry at the DIPROI end station using a thermopile positioned on the rear side of a Ge thin foil. Our scan covered the wavelength region 30-60 nm, thus confirming that FERMI can be effectively tuned on a relatively broad spectral range.
- January 20, 2012
Delivery of the elliptic mirror has been suspended and a temporary focusing set-up has been designed for RUN 10.

Jobs

- Post-doctoral position opening

Publication list

Highlights

- TIMEX peak temperature diagnostics published on PRL
- TIMEX pilot experiment on surface melting of S published on PRL
- Pilot experiments and TIMEX science
- Beam-shaping focusing capabilities
- WDM diagnostic device temperature

With the advent of 4th generation free electron laser (FEL) light sources, which provide ultra-short pulses and high photon numbers per pulse in the VUV to X-ray range, the study of matter under extreme conditions has become a major topic in condensed matter physics.

pdf